

Review

# Electrocoagulation as a Promising Defluoridation Technology from Water: A Review of State of the Art of Removal Mechanisms and Performance Trends

Milad Mousazadeh <sup>1,2,†</sup>, S. M. Alizadeh <sup>3</sup>, Zacharias Frontistis <sup>4</sup>, Işık Kabdaşlı <sup>5,†</sup>,  
Elnaz Karamati Niaragh <sup>6,†</sup>, Zakaria Al Qodah <sup>7</sup>, Zohreh Naghdali <sup>1,2</sup>, Alaa El Din Mahmoud <sup>8,9</sup>,  
Miguel A. Sandoval <sup>10,11</sup>, Erick Butler <sup>12</sup> and Mohammad Mahdi Emamjomeh <sup>13,\*</sup>



**Citation:** Mousazadeh, M.; Alizadeh, S.M.; Frontistis, Z.; Kabdaşlı, I.; Karamati Niaragh, E.; Al Qodah, Z.; Naghdali, Z.; Mahmoud, A.E.D.; Sandoval, M.A.; Butler, E.; et al. Electrocoagulation as a Promising Defluoridation Technology from Water: A Review of State of the Art of Removal Mechanisms and Performance Trends. *Water* **2021**, *13*, 656. <https://doi.org/10.3390/w13050656>

Academic Editor: Sergi Garcia-Segura

Received: 22 January 2021

Accepted: 24 February 2021

Published: 28 February 2021

**Publisher's Note:** MDPI stays neutral with regard to jurisdictional claims in published maps and institutional affiliations.



**Copyright:** © 2021 by the authors. Licensee MDPI, Basel, Switzerland. This article is an open access article distributed under the terms and conditions of the Creative Commons Attribution (CC BY) license (<https://creativecommons.org/licenses/by/4.0/>).

- <sup>1</sup> Student Research Committee, Qazvin University of Medical Sciences, Qazvin 34197-59811, Iran; m.milad199393@gmail.com (M.M.); zohreh.naghdali@gmail.com (Z.N.)
  - <sup>2</sup> Department of Environmental Health Engineering, School of Health, Qazvin University of Medical Sciences, Qazvin 34197-59811, Iran
  - <sup>3</sup> Petroleum Engineering Department, Australian College of Kuwait, West Mishref Safat-13015, Kuwait; s.alizadeh@ack.edu.kw
  - <sup>4</sup> Department of Chemical Engineering, University of Western Macedonia, GR-50132 Kozani, Greece; zfrontistis@chemeng.upatras.gr
  - <sup>5</sup> Environmental Engineering Department, Civil Engineering Faculty, İstanbul Technical University, Ayazağa Campus, Maslak 34469, İstanbul, Turkey; kabdasli@itu.edu.tr
  - <sup>6</sup> Civil and Environmental Engineering Department, Amirkabir University of Technology (Tehran Polytechnic), Hafez Ave., Tehran 15875-4413, Iran; elnazkaramati@gmail.com
  - <sup>7</sup> Department of Chemical Engineering, Faculty of Engineering Technology, Al-Balqa Applied University, Amman 19117, Jordan; zak@bau.edu.jo
  - <sup>8</sup> Environmental Sciences Department, Faculty of Science, Alexandria University, Alexandria 21511, Egypt; alaa-mahmoud@alexu.edu.eg
  - <sup>9</sup> Green Technology Group, Faculty of Science, Alexandria University, Alexandria 21511, Egypt
  - <sup>10</sup> Laboratorio de Electroquímica Medio Ambiental, LEQMA, Departamento de Química de los Materiales, Facultad de Química y Biología, Universidad de Santiago de Chile, USACH, Casilla 40, Correo 33, Santiago 9170022, Chile; ma.sandovallopez@ugto.mx
  - <sup>11</sup> Departamento de Ingeniería Química, División de Ciencias Naturales y Exactas, Universidad de Guanajuato, Noria Alta S/N, Guanajuato 36050, Guanajuato, Mexico
  - <sup>12</sup> School of Engineering, Computer Science, and Mathematics, West Texas A&M University, Box 60767, Canyon, TX 79016, USA; erick.ben.butler@gmail.com
  - <sup>13</sup> Social Determinants of Health Research Center, Research Institute for Prevention of Non-Communicable Diseases, Qazvin University of Medical Sciences, Qazvin 34199-15315, Iran
- \* Correspondence: m\_emamjomeh@yahoo.com  
† Co-first author, Milad Mousazadeh, Işık Kabdaşlı and Elnaz Karamati Niaragh contributed equally to this work.

**Abstract:** Fluoride ions present in drinking water are beneficial to human health when at proper concentration levels (0.5–1.5 mg L<sup>-1</sup>), but an excess intake of fluoride (>1.5 mg L<sup>-1</sup>) may pose several health problems. In this context, reducing high fluoride concentrations in water is a major worldwide challenge. The World Health Organization has recommended setting a permissible limit of 1.5 mg L<sup>-1</sup>. The application of electrocoagulation (EC) processes has received widespread and increasing attention as a promising treatment technology and a competitive treatment for fluoride control. EC technology has been favourably applied due to its economic effectiveness, environmental versatility, amenability of automation, and low sludge production. This review provides more detailed information on fluoride removal from water by the EC process, including operating parameters, removal mechanisms, energy consumption, and operating costs. Additionally, it also focuses attention on future trends related to improve defluoridation efficiency.

**Keywords:** electrocoagulation; groundwater treatment; water treatment; fluoride removal

## 1. Introduction

Fluoride anion is naturally found in the environment. Fluoride is released into groundwater from fluoride-containing minerals owing to interactions between water and rocks [1]. Fluoride concentrations in seawater, rivers, and groundwater have an average value of ca.  $1.0 \text{ mg L}^{-1}$ ,  $1.5 \text{ mg L}^{-1}$  and  $1.0\text{--}35.0 \text{ mg L}^{-1}$ , respectively [2]. Groundwater contamination by fluoride is a worldwide concern [3]. More than 70 countries report high concentration levels of fluoride in their drinking water sources. Most of these contaminated sources are found in South and Southeast Asia [4].

The permissible limit of fluoride in drinking water has been set by the World Health Organization (WHO) at  $1.5 \text{ mg L}^{-1}$  [5]. The human body requires low intake levels of fluoride to ensure enamel and bone formation, with suggested doses of  $1.0 \text{ mg L}^{-1}$ . However, fluoride contents over a maximum concentration level of  $1.5 \text{ mg L}^{-1}$  may induce deleterious health effects even at such a low concentration. A higher concentration of fluoride in drinking water has some adverse effects on human health, for instance, bioaccumulation in teeth and bones [6] neurological deterioration [7], and fluorosis [8,9]. Furthermore, fluoride in the gut may react with toxic elements such as lead and enhance their toxicity while digesting [3]. The health effects are summarized in Table 1 [4,10].

**Table 1.** Effects of fluoride on the health of humans [4,10].

Fluoride Concentration ( $\text{mg L}^{-1}$ )	Health Effects
<0.5	Increasing dental caries
0.5–1.5	Improving the bones and teeth strength
1.5–4	Children's dental fluorosis (molting in teeth)
>4	Dental and skeletal fluorosis (deformities in the bone)
>10	Incident of crippling fluorosis, thyroid disorder, infertility in women, cancer, and Alzheimer's syndrome

Different processes have been evaluated to reduce high fluoride concentrations in water and, consequently, to prevent hazardous health effects. Some examples of examined technologies include adsorption [11–13], chemical precipitation using lime or magnesium salts [14,15], co-precipitation and adsorption through coagulation–flocculation with alum [16,17], ion exchange [18,19], electro dialysis [20–22], and electrocoagulation [23,24]. Amongst these technologies, electrocoagulation (EC) has emerged in recent decades as a suitable alternative compared to the conventional coagulation process. EC is an electrically-driven water treatment having the potential to be implemented as a decentralized treatment unit. This treatment technology offers interesting merits as an eco-friendly option, including versatility, ease of setup, minimal sludge production without the need of chemical additives, and a small footprint without compromising the final water quality after treatment [25–27].

In this review paper, the fluoride removal mechanisms are explained and the defluoridation efficiency is scrutinized considering several factors such as solution characteristics, type of EC reactors, and operating parameters. Moreover, the importance of the residual aluminium concentration is highlighted. The fluoride removal from different synthetic and real groundwaters through alone and combined EC processes is studied together with the scaling-up of EC defluoridation plants located around the world. Finally, techno-economic analysis based on energy and electrode consumption is evaluated. This review is foreseen to gain attention of wider community including chemist, electrochemist, and environmental engineers interested in the elimination of fluoride using these technologies.

## 2. EC Fundamentals

### 2.1. Definition of Concepts

The EC process is considered as an advanced technology, associating three conventional water treatment pieces of knowledge, including electrochemistry, coagulation, and flotation [28,29]. This process is applicable for remediation of the industrial effluents and

groundwater, eliminating various pollutants before discharging or reusing the treated water. EC operation is conducted in electrolytic reactors consisting of at least two electrodes, which allow the current circulation through the external power supply. It is essential to highlight that the electrode surface serves to interexchange electrons with electroactive species in solution. The electro-dissolution of the sacrificial anode and the water reduction at the cathode yield coagulants species, which remove pollutants by forming large flocs that can be physically separated from water [29]. Coagulation and flocculation appear in consecutive steps, permitting particle collision and growth of floc. Coagulation results from the lessening of electrostatic repulsive forces, consequently, the negative charges ( $F^-$ ) are neutralized. Then, the suspended microscopic particles can stick together (not visible). Flocculation, a gentle mixing stage, helps to increase the size of the suspended particles into larger flocs (visible).

## 2.2. Theory and Principles of EC

The EC process relies on using an electrical current to generate in situ coagulants that enable different removal mechanisms of solutes and particles suspended in water. This technique consists of three stages: (i) in-situ electro-generation of aluminium or iron-based coagulants from sacrificial/consumable anodes made of Al or Fe, (ii) destabilizing pollutants through coagulant yielded, (iii) formation of flocs that can easily be separated from the water [26]. When the repulsive forces are neutralized, the suspended pollutants form larger particles that can settle down or float and adhered to rising hydrogen gas bubbles [28]. Oxidation and reduction reactions that transform pollutants to less toxic matter may occur during an EC process [30]. Derjaguin-Landau-Verwey-Overbeek (DLVO) theory may explain the formation of aggregates based on Van der Waals and double layer forces [31]. However, beyond DLVO, additional factors play crucial roles in stabilizing colloids, such as hydration and hydrophobic interactions. Based on similar application principles, the EC process can be applied to eliminating heavy metals, inorganic ions, dyes, tannins, organic matter, and suspended solids.

During an EC process, the flowing of electric current through the immersed electrodes causes the dissolution of the anode to generate  $Al^{3+}$  or  $Fe^{2+}/Fe^{3+}$  ions. Simultaneously, the cathode generates hydroxide ( $OH^-$ ) ions and hydrogen ( $H_2$ ) gas from the water reduction reaction [26]. The related reactions, which depended on the solution characteristics, are presented briefly in Equations (1) and (2) (which occurs at the anode), Equations (3) and (4) (occurring at the cathode), and in Equations (5)–(7) (in the bulk solution) [26].

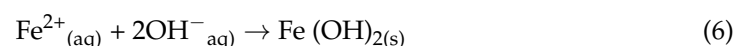
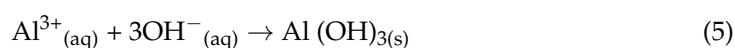
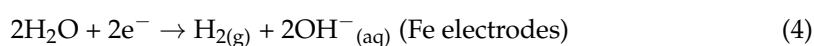
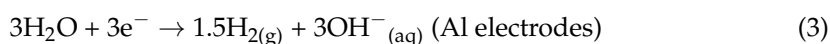


Figure 1 illustrates the general mechanisms that occur during the EC process involving electro-generation of coagulants, coagulation, flocculation, precipitation, and/or flotation [26,32]:

Charge neutralization of the ionic species occurs by the effect of the counter ions, which are generated at the sacrificial anode. These cations diminish the repulsive electrostatic force between particles where the van der Waals force of attraction predominates, lessening the surface potential and the energy impediment required to form the aggregate and causing coagulation (A zero net charge is the result). After that, the suspended small

particles connect each other to form large-sized and long-chain flocs. Finally, those particles can be removed by sedimentation (sweep coagulation) or flotation.

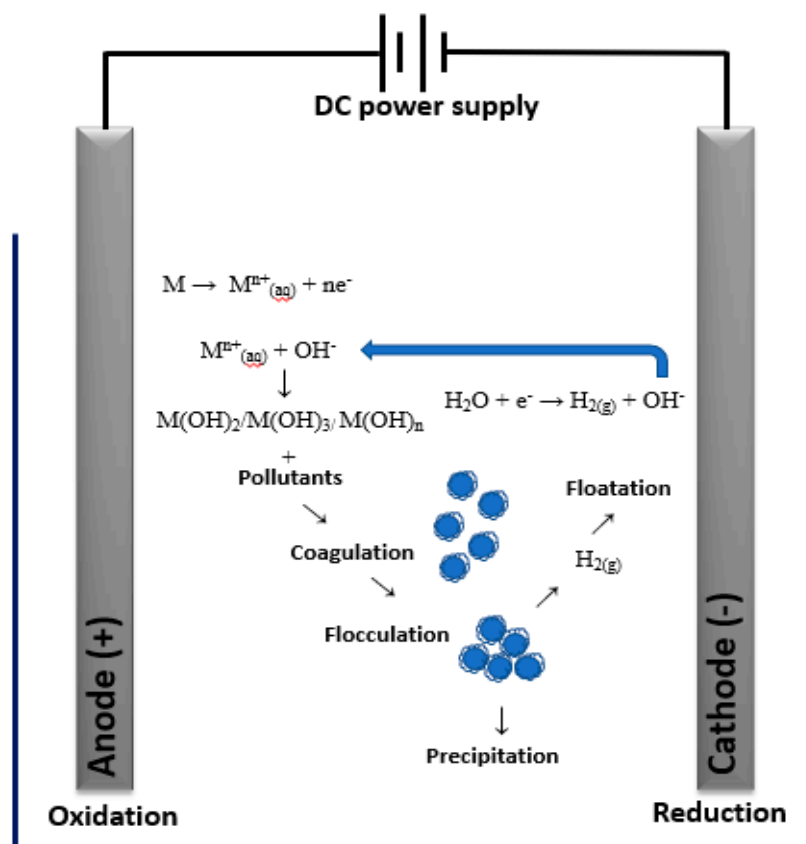


Figure 1. Electrocoagulation process mechanisms.

### 2.3. Pros and Cons of EC

The EC process is an electrochemically driven technology that entails several major benefits: environmental compatibility, versatility, amenability, and cost-effectiveness over conventional biological processes or chemical treatment methods. Energy requirements can be covered by renewable energy sources (e.g., solar energy), which allow deployment off-grid as green sustainable technology. Despite the mentioned pros, the EC process has major cons such as electrode passivation and electrical energy costs, limiting competitive applications for groundwater treatment under specific case scenarios [26,28,30]. The crucial pros and cons of the EC technique are summarized in Table 2. However, research teams have tried to evaluate some solutions to overcome the challenges of EC technology. For instance, the alternating current (AC) may reduce electrode passivation. Passivation is the formation of an inert oxide layer on the electrode/electrolyte interface that inhibits the electro-dissolution and increases the cell potential, which augments the energy consumption [30]. Mao et al. [33] concluded that alternating pulse current helps prevent the passivation of Al anode during the electrolysis and avoids the extra energy consumption for the resistance of aluminium oxide film formed on the anode surface. Karamati Niaragh et al. [34] also reported the AC effectiveness in decreasing electrode passivation extent resulted in diminishing the EC operating costs.

**Table 2.** Pros and cons of electrocoagulation (EC) technique [32,33,35].

Pros.	Cons
<b>Green technology</b>	<b>Electrode passivation</b>
✓ No need for adding chemicals in comparison with chemical coagulation which reduces secondary pollution release	✗ Formation of an oxide film on the surface of the electrode during the electrolysis
✓ Volume of produced sludge decreased	✗ Reduction of the anode dissolution which in turn reduces the removal efficiency of pollutants
✓ Possible recovery of hydrogen gas to be used as fuel	✗ Results in higher costs of electricity
<b>Environmental compatibility</b>	<b>Regular sacrificial anode replacement</b>
✓ Removal of very small particles, as the fine charged particles are more easily attracted to the electric field	✗ It influences the operating costs
<b>Amenability to automation</b>	<b>High conductivity requirement</b>
✓ It has potential to be operated in a complete automation way due to its equipment's simplicity	<b>High electrical energy costs</b>
✓ Produced gas bubbles floats the pollutants which facilitates their removal	✗ It may limit application in countries with higher costs of electrical energy; but can be minimized using renewable energy resources such as solar panels
✓ It produces larger flocs being easily separated by filtration compared with coagulation	

### 3. Fluoride Removal Mechanisms

The EC process using aluminium electrodes has been a well-studied defluoridation process for drinking water and groundwaters. The EC process with aluminium electrodes attains high fluoride removal efficiencies. On the other hand, a limited number of studies focused on defluoridation by the EC technique utilizing iron or stainless steel electrodes from synthetically prepared samples [36–40]. The main reason for this lack of studies is the low removal performance observed when using iron-based sacrificial electrodes. The notorious difference between Al and Fe electrodes may be explained by the differentiate removal mechanism that induces water defluoridation. In this section, the removal mechanisms are defined and introduced in detail.

During the EC process,  $\text{Al}^{3+}$  is generated through anodic dissolution (Equation (1)). Electro-dissolved  $\text{Al}^{3+}$  is hydrated to  $\text{Al}(\text{H}_2\text{O})_6^{3+}$  yielding monomeric, dimeric, and polymeric species such as  $\text{Al}(\text{H}_2\text{O})_4(\text{OH})^{2+}$ ,  $\text{Al}(\text{H}_2\text{O})_5(\text{OH})^{2+}$ ,  $\text{Al}(\text{OH})^{2+}$ ,  $\text{Al}(\text{OH})_2^+$ ,  $\text{Al}(\text{OH})_4$ ,  $\text{Al}_2(\text{OH})_2^{4+}$ ,  $\text{Al}_6(\text{OH})_{15}^{3+}$ ,  $\text{Al}_7(\text{OH})_{17}^{4+}$ ,  $\text{Al}_8(\text{OH})_{20}^{4+}$ ,  $\text{Al}_{13}(\text{OH})_{34}^{5+}$ , and  $\text{Al}_{13}\text{O}_4(\text{OH})_{24}^{7+}$  through a series of polymerization reactions in the bulk solution [30,41–45]. These monomeric and polymeric aluminium hydroxo complexes lately induce the production of amorphous  $\text{Al}(\text{OH})_3(\text{H}_2\text{O})_3$  (sweep-flocs) with large surface areas. Flocs are capable of trapping colloidal particles and adsorbing soluble compounds. The freshly formed flocs are ultimately polymerized to  $\text{Al}_n(\text{OH})_{3n}$  at high aluminium concentrations [41,46]. The transformation reactions for in-situ formed aluminium in the EC process are similar to those of conventional alum coagulation shown in Figure 2 [43].

The formation of aluminium hydroxo complexes is strongly pH-dependent. In the pH range between 4 and 8, the positively charged poly-hydroxo complexes such as  $\text{Al}_8(\text{OH})_{20}^{4+}$  and the amorphous solid  $\text{Al}(\text{OH})_3(\text{H}_2\text{O})_3$  dominates in the solution [41]. The polymeric hydroxo complex species play an important role in the destabilization of negatively charged particles and solutes (i.e., fluoride) through charge neutralization. At alkaline pH with values higher than 8.0, aluminium solubility increases owing to increasing concentration of negatively charged  $\text{Al}(\text{OH})_4^-$  and  $\text{AlO}_2^-$  and destabilization capacity for negatively charged colloids decreases [30,46].

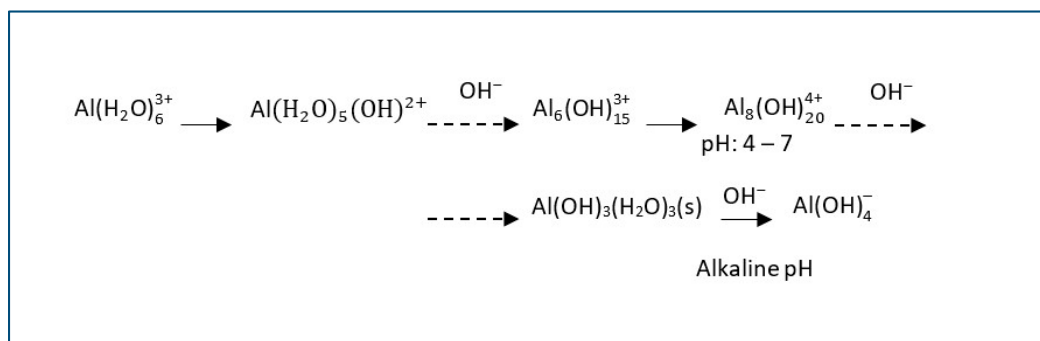


Figure 2. Polymerization reactions of aluminium. Modified after Rebhun and Lurie [43].

Defluoridation performance reported in the literature for the EC process are superior to that of conventional alum coagulation owing to the electro-condensation effect. This effect is attributed to an increase in fluoride concentration near to the anode in bulk solution because of electrostatic attraction of negatively charged fluoride ions.

Fluoride removal by the EC process using aluminium sacrificial anodes takes place via (i) adsorption on the formed aluminium hydroxide flocs, (ii) co-precipitation, (iii) fluoride attachment to electrodes, and/or (iv) precipitation of insoluble cryolite ( $\text{Na}_3\text{AlF}_6$ ;  $K_{\text{so}} = 10^{-33.84}$ ).

Adsorption is one of the fluoride removal mechanisms that realize by the substitution of hydroxyl groups present in the aluminium flocs by fluoride ions to form  $\text{Al}_n\text{F}_x(\text{OH})_{3n-x}\text{(s)}$  according to the following reaction:



The formation of  $\text{Al}_n\text{F}_m(\text{OH})_{3n-m}$  increases pH due to the release of hydroxyl ions into the solution [47]. In slightly alkaline solutions, fluoride is released into the solution to form either F-free  $\text{Al(OH)}_3$  or  $\text{Al(OH)}_4^-$  due to the limited stability of  $\text{Al}_n\text{F}_m(\text{OH})_{3n-m}$ . Thus, the optimum pH range for fluoride removal by adsorption is considered as 6–7. Figure 3 schematically illustrates the reaction pathway for fluoride removal via adsorption.

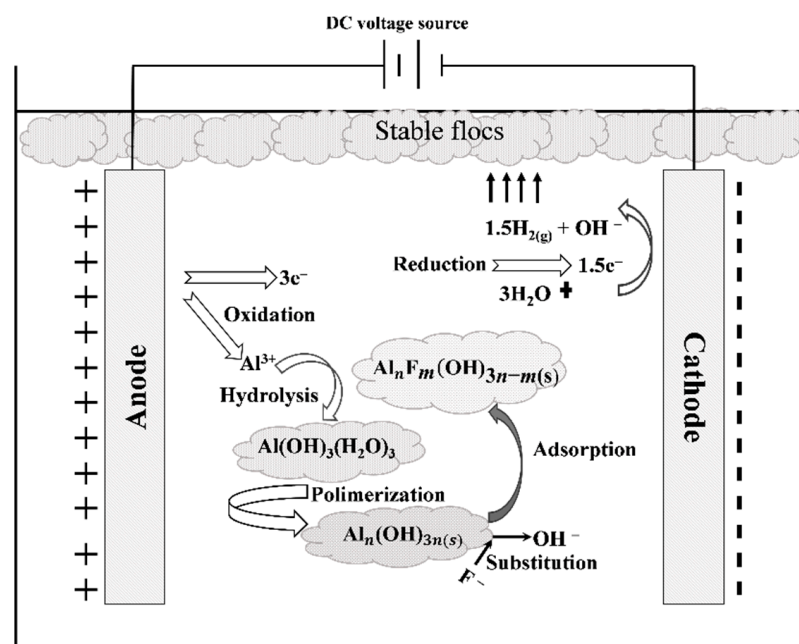
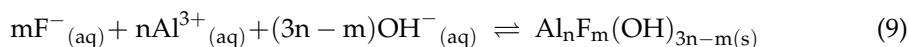


Figure 3. Fluoride removal via the adsorption on the aluminium hydroxide flocs.

Removal of fluoride by co-precipitation is based on the direct formation of insoluble  $\text{Al}_n\text{F}_m(\text{OH})_{3n-m}$  by the reaction given as follows.



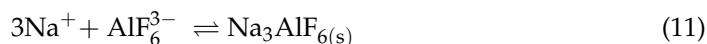
The insoluble  $\text{Al}_n\text{F}_m(\text{OH})_{3n-m}$  produced through either adsorption or co-precipitation process is easily separated from water by physical means such as flotation and filtration. The formation of the insoluble  $\text{Al}_n\text{F}_m(\text{OH})_{3n-m}$  has been confirmed by several chemical analyses of the sludge produced during the EC process [41,44,48,49].

The attachment of fluoride on the electrodes resulting from the electrophoresis and/or electro-condensation effects in the electric field is another fluoride removal mechanism [50]. This mechanism is explained using a hypothetical hydro-fluoro-aluminium complex  $\text{Al}_n(\text{OH})_m\text{F}_k^{3n-m-k}$  (HFA). At  $3n = m + k$ , HFA complexes present as insoluble particles can be eliminated from water by filtration. At  $3n < m + k$ , the negatively charged HFA move towards anode by electromigration and are adsorbed at the anode surface. Contrary, at  $3n > m + k$ , the positively charged HFA are attracted to the cathodic side by electrophoretic effect and then neutralize with hydroxyl ions liberated near the cathode to form colloidal flocs attached on the cathode surface. When anode and cathode are taken out of the EC reactor, this gelatinous layer attached to them is removed. This mechanism's contribution to overall defluorination efficiency seems to be highly dependent on the operation conditions such as pH, charge loading, current density, and initial fluoride concentration [46,50,51].

Fluoride ions may form strong complexes with aluminium.  $\text{AlF}_6^{3-}$  is one of these fluoro-aluminium complex species which may form near the anode, where both  $\text{F}^-$  and  $\text{Al}^{3+}$  ions present in high concentrations:



Subsequently,  $\text{AlF}_6^{3-}$  transforms into cryolite during the EC process if the solution pH is kept around 5–6 [46,52,53]. This transformation is represented as follows:



The formation of cryolite through the EC process with aluminium electrodes depends on reaction conditions such as solution pH and Al/F molar ratio and sodium concentration applied. Cryolite crystals can be removed or recovered. In addition to the above-mentioned solid phases, some cations such as  $\text{Ca}^{2+}$ ,  $\text{Mg}^{2+}$ , or  $\text{Fe}^{2+}$  existing in water to be treated by EC technique may transform into insoluble fluoride solid phases in bulk solution. Depending on initial fluoride and calcium concentrations,  $\text{Ca}^{2+}$  may precipitate as insoluble  $\text{CaF}_2$  [54–56]:

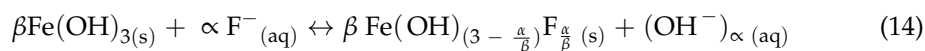


or may co-precipitate together with  $\text{Al}^{3+}$  [57]:

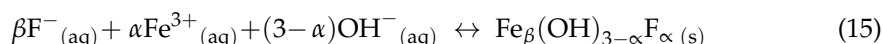


It is evident from the published data that either the formation of insoluble  $\text{CaF}_2$  or incorporation of  $\text{Ca}^{2+}$  into aluminium hydroxide has a positive effect on defluorination efficiency in the EC process. Similar to calcium, insoluble  $\text{MgF}_2$  may also be formed in the presence of  $\text{Mg}^{2+}$  [53,55,56].

Amarasooriya and Kawakami [37] claimed that fluoride removal mechanisms are as sweep coagulation (adsorption) and the enmeshment of fluoride ions by insoluble ferric hydroxide precipitate (co-precipitation) in the bulk solution similar to the usage of aluminium anodes. Fluoride adsorption in bulk solution:



Fluoride co-precipitation in bulk solution:



Das and Nandi [58] used Equations (14) and (15) for simultaneous removals of fluoride and ferrous ions from the synthetically prepared sample (NaF+FeSO<sub>4</sub>·7H<sub>2</sub>O in tap water) by electrocoagulation using aluminium electrode to clarify the effect of the co-existing cation of Fe<sup>2+</sup> on process efficiency.

In a few studies, it was suggested that insoluble FeF<sub>3</sub> may precipitate as a result of a substitution reaction between fluoride anions and hydroxyl groups existing in the freshly formed Fe(OH)<sub>3</sub> [36,59] according to the following reaction:



It should be pointed out that any solid analysis did not present in order to support the aforementioned removal mechanisms expressed by Equations (14)–(16).

It is worth mentioning that adsorption taking place substitution of hydroxide groups present in Al<sub>n</sub>(OH)<sub>3n</sub> flocs by the fluoride ions is the most prevalent fluoride removal mechanism for the EC using aluminium anodes [36,41,42,44,46–48,50–53,55,56,60–67]. Co-precipitation of fluoride and hydroxide ions with aluminium ions to produce a precipitate, Al<sub>n</sub>F<sub>m</sub>(OH)<sub>3n–m</sub> is another mechanism occurring together with the adsorption [36,42,44,46–48,50,53,55,56,68]. The formation of Al<sub>n</sub>F<sub>m</sub>(OH)<sub>3n–m</sub> has already been confirmed by the results of scanning electron microscopy (SEM), X-ray energy dispersive analysis (EDX), X-ray diffraction (XRD), fourier transform infrared spectrophotometer (FTIR), and time-of-flight secondary ion mass spectroscope system (ToF-SIMS) analyses conducted on the flocs produced during the EC process. Analyses of both anode and cathode by using EDX and X-ray photoelectron spectroscopy (XPS) have verified the defluoridation by the attachment of fluoride on the aluminium electrodes [38,44,50,51]. Over 50% of the total fluoride was attached to the electrodes at an optimum pH of 6.5. A few scientific studies confirmed the formation of cryolite and Al<sub>n</sub>F<sub>m</sub>(OH)<sub>3n–m</sub> flocs [46,52,53]. Nevertheless, the fluoride removal mechanism has been demonstrated as the competitive Adsorption between OH<sup>–</sup> and F<sup>–</sup> in these studies. Until now, only limited data is available in the literature dealing with defluoridation by electrocoagulation using iron or stainless steel electrodes. Therefore, further studies are necessary to elucidate the fluoride removal mechanisms and their roles on the defluoridation process.

#### 4. Adsorption Kinetics

The defluoridation rate depends on several operation parameters such as the initial fluoride concentration, pH, and the current density. In general, it follows the pseudo-first or second-order kinetics. The pseudo-first-order kinetics for defluoridation is represented as below:

$$\ln \frac{[F_t]}{[F_o]} = -k_1 \times t \quad (17)$$

where F<sub>o</sub> and F<sub>t</sub> are the fluoride concentrations (in mol L<sup>–1</sup>) at the initial and at a certain EC time, respectively. t is the EC treatment time, and k<sub>1</sub> is the pseudo first order reaction rate constant. The following equation expresses the pseudo second order reaction for defluoridation:

$$\frac{1}{[F_t]} - \frac{1}{[F_o]} = k_2 \times t \quad (18)$$

where k<sub>2</sub> is the pseudo-first-order reaction rate constant.

The data obtained for the adsorption of fluoride ions onto aluminium hydroxide flocs generated in the EC process satisfactorily agree with both the pseudo-first-order kinetics [41,69] and the pseudo second-order kinetics [44,58,61]. The defluoridation rates derived from the pseudo-order kinetics are dependent on the reaction conditions. As is evident in Table 3, the pseudo second-order defluoridation rate constant significantly

changes with critical parameters such as the current density, the current concentration (I/V), the initial fluoride concentration, or/and the EC operation time. On the other hand, the pseudo first-order defluoridation rate constants obtained for similar EC operation conditions are the same magnitude.

**Table 3.** The pseudo-order defluoridation rate constants ( $R^2 \geq 0.95$ ).

	$k (\times 100)$	$F_o (\text{mg L}^{-1})$	Operation Conditions	Ref
$k_1$	3.6–6.1	10	pH 6–8; I/V: 273–683 A m <sup>-3</sup> ; 10 mS m <sup>-1</sup> ; 60 min DC	[70]
$k_1$	3.35–5.8	15	pH 6–8; I/V: 273–683 A m <sup>-3</sup> ; 10 mS m <sup>-1</sup> ; 60 min DC	[70]
$k_1$	2.7–5.7	25	pH 6–8; I/V: 273–683 A m <sup>-3</sup> ; 10 mS m <sup>-1</sup> ; 60 min DC	[70]
$k_1$	3.17–7.21	10	pH <sub>o</sub> 7; 1.5–12.93 mA cm <sup>-2</sup> ; 60 min; Fe (10 mg L <sup>-1</sup> ); DC	[58]
$k_2$	6.29–3.91	3–12	pH <sub>o</sub> 6; 0.27 mA cm <sup>-2</sup> ; 30 min; DC	[61]
$k_2$	0.17995–0.33954	5–20	pH <sub>o</sub> 7; 10 mA cm <sup>-2</sup> ; 300 min; AC	[71]
$k_2$	0.16846–0.24659	5–20	pH <sub>o</sub> 7; 10 mA cm <sup>-2</sup> ; 300 min; DC	
$k_2$	1.4	12	pH <sub>o</sub> 7; 1 mA cm <sup>-2</sup> ; 95 min; DC	[44]
$k_2$	0.6	12	pH <sub>o</sub> 7; 1 mA cm <sup>-2</sup> ; 95 min; As (550 µg L <sup>-1</sup> ); DC	[44]

k: in min<sup>-1</sup> and mg<sup>-1</sup> L<sup>-1</sup> for the pseudo 1st and 2nd order reaction kinetics.

Furthermore, the variable order kinetic (VOK) model is defined as a combination of the pseudo first-order kinetics and Langmuir adsorption isotherm. In this model, the amount of aluminium hydroxide formed during electrocoagulation is incorporated into the defluoridation rate equation as follows [68]:

$$-\frac{d[F]}{dt} = \varepsilon_{Al} \times \varepsilon_C \times \frac{n \times I}{Z \times F \times V} \times \frac{\Gamma_{\max} \times k_L \times [F]}{1 + k_L \times [F]} \quad (19)$$

where  $\varepsilon_{Al}$  and  $\varepsilon_C$  are the efficiencies (%) of hydrofluoro aluminium formation and the current, respectively.  $n$  is the number of cell;  $I$  is the applied current (A);  $Z$  is the valence of the metal of the anode (=3 for aluminium);  $F$  is the Faraday constant (96,500 C);  $V$  is the working volume of the water (L);  $\Gamma_{\max}$  represents the maximum amount of fluoride removed per mole of Al<sup>3+</sup> at a given pH; and  $k_L$  is the Langmuir constant (L mol<sup>-1</sup>). The order of defluoridation rate expressed by Equation (19) is variable. In the case of  $k_L^{-1} \gg [F]$ , it obeys first-order kinetics. The VOK model turns to zero-order kinetics if  $k_L^{-1} \ll [F]$ .

Hu et al. [68] reported that (i)  $\Gamma_{\max}$  and  $k$  were constant when the initial fluoride concentration varied from 15 to 25 mg L<sup>-1</sup>; (ii)  $\varepsilon_C$  varied with the current density and should be accurately determined, and (iii) the fitness to the data obtained from the VOK model was very satisfactory except the system with an initial acidity of 0.5 and 1.0 mM together with high fluoride concentrations.

A modification of the VOK model coupled with Langmuir and Freundlich adsorption isotherms is also available for defluoridation in the literature [41,72].

$$-\frac{d[F]}{dt} = \varepsilon_{Al} \times \varepsilon_C \times \frac{n \times I}{Z \times F \times V} \times \frac{\Gamma_{\max} \times k_{LF} \times [F]^n}{1 + k_{LF} \times [F]^n} \quad (20)$$

Table 4 summarizes the VOK parameters according to the literature. As seen in the table, the calculated Langmuir ( $k_L$ ) and Langmuir-Freundlich ( $k_{LF}$ ) as well as  $\Gamma_{\max}$  values are comparable and the same magnitude.

For a target fluoride concentration;  $[F]_t$ , the EC retention time ( $t_N$ ) required is obtained from the integral form of Equation (19) [68]:

$$t_N = \frac{Z \times F \times V}{\varepsilon_{Al} \times \varepsilon_C \times n \times I \times \Gamma_{\max}} \left( [F]_o - [F]_t + \frac{1}{k} \times \ln \frac{[F]_o}{[F]_t} \right) \quad (21)$$

**Table 4.** The VOK model parameters.

	$k$ (L mol <sup>-1</sup> )	$\Gamma_{\max}$	Operation Condition	Ref
$k_L$	1520	0.474	pH <sub>0</sub> 5.2; 0.025–0.4 A; F <sub>0</sub> 25 mg L <sup>-1</sup> ; Cl <sup>-</sup> 5 mM	[68]
$k_L$	1520	0.549	pH <sub>0</sub> 5.2; 0.4 A; F <sub>0</sub> 15–25 mg L <sup>-1</sup> ; Cl <sup>-</sup> 5 mM	[68]
$k_{LF}$	1600 ± 9.8	0.75 ± 13	pH <sub>0</sub> 7; 17.1 mA cm <sup>-2</sup> ; F <sub>0</sub> 0.33–1.05 mM, 7.5 mS m <sup>-1</sup>	[73]
$k_{LF}$	1675	0.9	pH <sub>0</sub> 7; 17.1 mA cm <sup>-2</sup> ; F <sub>0</sub> 15 mg L <sup>-1</sup> , 7.5 mS m <sup>-1</sup>	[72]

Equation (21) proposed by Hu et al. [68] and its modified form adopted to the Langmuir and Freundlich isotherms were used to calculate  $t_N$  for a continuous-flow bipolar EC reactor [74], an airlift EC reactor [73] and an external-loop airlift EC reactor [72].

Defluoridation efficiency is strongly dependent on the design, configuration, and operation mode of the EC reactor and the nature and characteristics of the pollutant to be treated. The above-mentioned kinetics data were obtained from the experimental studies performed using EC reactors with different design and operated on lab-scale mode using the synthetically prepared samples. The studies on natural waters are quite limited. Therefore, further studies are required to improve engineering design and full-scale application.

### 5. Factors Influencing the EC Process Efficiency in Defluoridation

According to several studies on fluoride removal via the EC process, various parameters affect the removal efficiency. As a holistic approach, the affecting parameters are classified into two major categories: (i) physicochemical solution characteristics and (ii) operational parameters related to reactor design. All operational parameters and solution characteristics given in Figure 4 might influence the EC process performance. A summary of some evaluated factors and conditions with defluoridation performance using EC system is presented in Table 5.

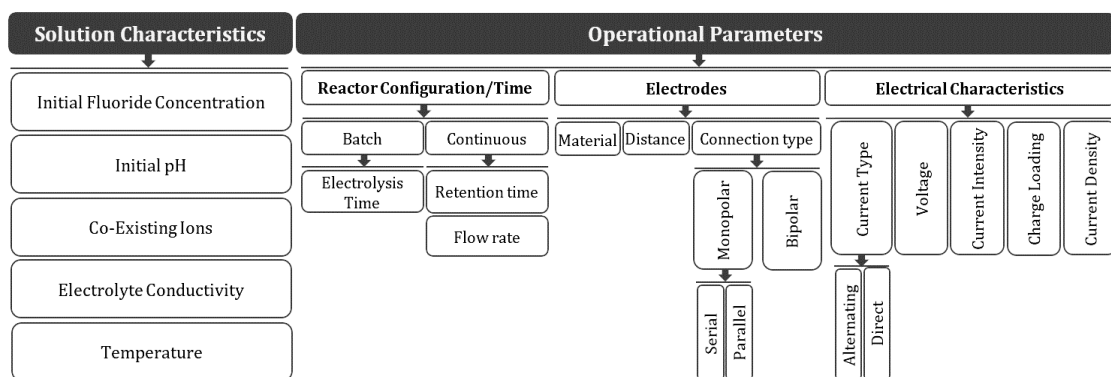


**Figure 4.** A comprehensive look at operational parameters and solution characteristics that affect an EC process performance.

As is shown in Figure 5, the EC process with various operational conditions and solution characteristics has been a useful process to achieve high removal fluoride efficiencies (<99%) with different initial concentrations (0–50 mg L<sup>-1</sup>). According to the literature, Al electrodes have been mostly applied in removing fluoride due to their effectiveness [57,59]. In recent years, the EC process was redesigned to remove other pollutants such as arsenic [10], hydrated silica [62], and iron [67] alongside fluoride. The EC process was also used in combination with other methods such as microfiltration [75] to techno-economically remove fluoride; further explanation of the parameters most influential on fluoride removal using the EC process is presented accordingly.

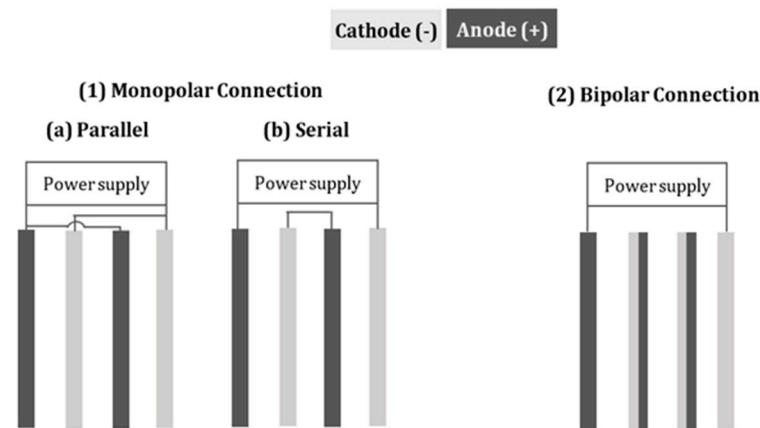


Figure 5. Various connection types of electrodes to the power supply in an electrocoagulation process.

Table 5. Summary of some evaluated factors and defluoridation efficiency using EC process (\* defluoridation).

Year	Evaluated Factors and Conditions	Cathode-Anode/ Connection Type	Optimum	Efficiency * (%)	Ref
2020	Initial pH (5–9) Current density (1.5–12.93 mA cm <sup>-2</sup> ) Electrolysis time (60 min) NaCl concentration (0.33–0.83 g L <sup>-1</sup> ) Inter-electrode distance (1–2.5 cm) Initial F concentration (0–25 mg L <sup>-1</sup> )	Al-Al Monopolar	7 4.31 mA cm <sup>-2</sup> 60 min 0.33 g L <sup>-1</sup> 1 cm 10 mg L <sup>-1</sup>	96%	[58]
2020	Current density (4–7 mA cm <sup>-2</sup> ) Mean linear flow rate (1.2–4.8 cm s <sup>-1</sup> )	Al-Al	7 mA cm <sup>-2</sup> 1.2 cm s <sup>-1</sup>	<80%	[60]
2019	Initial F concentration (5–50 mg L <sup>-1</sup> ) Temperature (25–55 °C) Conductivity (1–6 mS/cm) Initial pH (4–8.5)	Al-Al Monopolar	-	90%	[47]
2019	Current density (3–10 mA cm <sup>-2</sup> ) Electrolysis time (5–15 min) Polarity half-period (0.5–2 min)	Al-Al Monopolar	10 mA cm <sup>-2</sup> 15 min	85.9 %	[74]
2019	Current density (0.5–4.5 mA cm <sup>-2</sup> ) Initial F concentration (5–10 mg L <sup>-1</sup> ) Initial As concentration (40–80 µg L <sup>-1</sup> ) Electrolysis time (5–15 min)	Al-Al & Fe-Fe Monopolar	4.5 mA cm <sup>-2</sup> 5 mg L <sup>-1</sup> 80 µg L <sup>-1</sup> 15 min	85.68%	[10]
2019	Initial F concentration (6.02–8.98 mg L <sup>-1</sup> ) Electrolysis time (5–30 min) Initial pH (1.04–11.20) Current density (3–15 mA cm <sup>-2</sup> ) Voltage reversal (30–120 s)	Al-Al Monopolar	-	<93.91%	[42]
2018	Initial F concentration (1.78–7.89 mg L <sup>-1</sup> ) Current density (5–15 mA cm <sup>-2</sup> ) Initial pH (3.86–11.28)	Al-Al Bipolar	-	<99.45%	[76]
2017	Initial F concentration (10–20 mg L <sup>-1</sup> ) Current density (1–3 mA cm <sup>-2</sup> ) Initial pH (4–8) Inter-electrode distance (0.5–1.1 cm) Electrolysis time (0–30 min)	Al-Al (perorated discoind)	4.31 2 mA cm <sup>-2</sup> 6 0.5 cm 25 min	98%	[77]
2016	Flow rate (0.91–1.82 cm s <sup>-1</sup> ) Current density (4,5,6 mA cm <sup>-2</sup> ) Ions effect (Ca <sup>2+</sup> , SO <sub>4</sub> <sup>2-</sup> , Mg <sup>2+</sup> , PO <sub>4</sub> <sup>3-</sup> )	Al-Al	-	76–94%	[63]

Table 5. Cont.

Year	Evaluated Factors and Conditions	Cathode-Anode/ Connection Type	Optimum	Efficiency * (%)	Ref
2015	Charge loading (0–1700 CL <sup>-1</sup> ) Electrolysis time (45 min) Current density (2.17–13.2 mA cm <sup>-2</sup> ) Electrode material (Fe and Al) Effect of ions (Ca <sup>2+</sup> , Mg <sup>2+</sup> , Al <sup>3+</sup> )	Fe-Fe Al-Al Monopolar	-	<90% (Fe) <99% (Al)	[55]
2011	Initial F concentration (25–125 mg L <sup>-1</sup> ) Current density (0–0.0333 A cm <sup>-2</sup> ) Electrolysis time (5–25 min) Initial pH (3–11)	Al-Al Monopolar	- 25 mg L <sup>-1</sup> - 0.0111 A cm <sup>-2</sup> - 25 min - 7	90%	[41]
2009	Current density (12.5–50 A m <sup>-2</sup> ) Flow rate (150–400 mL min <sup>-1</sup> ) Initial F concentration (5–25 mg L <sup>-1</sup> ) Initial pH (4–8)	Al-Al Monopolar	Residence time (20–53 min)	<95%	[48]
2007	Initial F concentration (3–15 mg L <sup>-1</sup> ) Initial pH (5.5–8) Charge loading (0.52–4.15 Faraday m <sup>-3</sup> ) Current density (4.63–92.59 A m <sup>-2</sup> )	Al-Al Monopolar	-	<95%	[50]

### 5.1. Solution Characteristics

#### 5.1.1. Initial Fluoride Concentration

The initial fluoride concentration is a significant factor in EC process performance. Even though the relationship between removal efficiency and initial fluoride concentration is not simple, higher initial fluoride concentration in most cases requires longer operation times to achieve similar final concentration goals than the required for lower initial concentrations. Regarding this issue, Hashim et al. [77] identified adsorption of fluoride on metallic hydroxide flocs as the prominent step of the removal pathway when a higher initial fluoride concentration is present. Also, the EC process required larger amounts of aluminum flocs to be available. Thus, more electrolysis time in constant current density is required to produce higher amounts of aluminium hydroxide flocs in the bulk solution. Emamjomeh and Sivakumar [70] also reported the same results for fluoride removal using a batch reactor. Zhu et al. [50] indicated that flocs' removal efficiency and capacity improved by increasing the initial fluoride concentration.

#### 5.1.2. Initial pH

The raw water's initial pH is considered a crucial parameter that affects the EC process performance for fluoride elimination. As discussed in EC's fundamental principles, the formation of polymeric-hydroxo complexes of aluminium is highly dependent on the pH value [44]. Thereby, fluoride removal capacity is impacted. It is true that during the electrolytic process, pH can be altered due to hydroxide ions production at the cathode but decreases overall system performance until EC reaches optimum pH conditions.

Emamjomeh et al. [46] studied the effects of a wide range of initial pH from 2 to 10 on fluoride removal. At a pH of 2, the formation of Al(OH)<sub>3</sub> flocs was not observed, leading to a decline in the removal efficiency. They found that at the final pH of more than 6 the fluoride elimination reached values over 92%, which was achieved within an initial pH range between 3 to 8. Independently of the initial condition, the final pH of solution augmented to 8.5–8.9 due to the buffering capacity of Al(OH)<sub>3</sub>/Al(OH)<sub>4</sub><sup>-</sup>. At pH of 9 and higher, Al(OH)<sub>4</sub><sup>-</sup> and AlO<sub>2</sub><sup>-</sup> were formed, which are of no use in fluoride removal. Formation of these soluble species decreases the availability of flocs and the removal performance of

the system. Similar results were confirmed by Oulebsir et al. [78]. Das and Nandi [58] reported 7.0 as the optimum pH for higher removal efficiency. Thus, pH adjustment can contribute to optimizing removal efficiency but is not strictly required. The EC can be applied with considerable efficiency in a wide range of initial pH conditions. Here, the importance of effluent pH obtained at the end of the EC process must be emphasized in terms of remaining aluminium, which sometimes depends on the effluent pH (pH < 5; pH > 8.6).

#### 5.1.3. The Presence of Co-Existing Ions

Another important solution characteristic is the presence of other common ions found in natural waters such as sulfate ( $\text{SO}_4^{2-}$ ), phosphate ( $\text{PO}_4^{3-}$ ), chloride ( $\text{Cl}^-$ ), nitrate ( $\text{NO}_3^-$ ), calcium ( $\text{Ca}^{2+}$ ), and magnesium ( $\text{Mg}^{2+}$ ) [55,56,63,79]. The co-existence of other anions competes with fluoride decreasing fluoride migration to the anode surface; hence, fluoride removal efficiency may be affected by co-existing anions. Considering this competing effect and higher affinity of fluoride and sulfate ions with  $\text{Al}^{3+}$ , Hu et al. [79] reported that the impact of  $\text{SO}_4^{2-}$  on defluoridation was significant. Similar results for  $\text{PO}_4^{3-}$  and  $\text{SO}_4^{2-}$  were also reported by Un et al. [56]. However, the presence of  $\text{Cl}^-$  and  $\text{NO}_3^-$  did not influence the fluoride removal efficiency [55]. As mentioned in Section 3, the presence of  $\text{Ca}^{2+}$  and  $\text{Mg}^{2+}$  act as a suitable coagulant may improve the fluoride removal efficiency due to co-precipitation reactions between fluoride and these cations [55,56].

#### 5.1.4. Electrolyte Conductivity

In an electrochemical process such as EC, the electrolyte conductivity is crucial due to its role in determining the cell resistance and its effects on the electrode and bulk solution reactions. Adding supporting electrolyte reduces the energy consumption by reduction of ohmic resistance [56]. Hashim et al. [77] found that adding supporting electrolytes to increase water conductivity from 0.2 to 1  $\text{mS cm}^{-1}$  resulting in a significant reduction of energy consumption from 3.7 to 0.79  $\text{kWh m}^{-3}$  and a reasonable improvement of fluoride removal efficiency. However, the co-existence of other ionic species may affect removal performance, as discussed above. Un et al. [56] applied various  $\text{Na}_2\text{SO}_4$  concentrations to evaluate its impact on fluoride removal during the EC process (1  $\text{mA cm}^{-2}$ ). Results demonstrated that higher  $\text{Na}_2\text{SO}_4$  concentrations (>0.01 M) decreased fluoride removal efficiency due to the competitive effect of extra excess  $\text{SO}_4^{2-}$  ions despite the conductivity enhancement. Conversely, more electricity was consumed in lower conductivity solutions (0.01 M  $\text{Na}_2\text{SO}_4$  concentration with 5.88  $\text{kW m}^{-3}$  and 0.03 M  $\text{Na}_2\text{SO}_4$  concentration with 2.77  $\text{kW m}^{-3}$ ). Thakur and Mondal [80] used NaCl as a cheap and low toxicity-supporting electrolyte; a NaCl concentration augmentation from 0.5 to 0.71  $\text{g L}^{-1}$  improved fluoride removal efficiency and reduced operating cost due to less energy consumption. Grich et al. [47] evaluated conductivity of solution using NaCl on fluoride removal. This electrolyte does not compete with fluoride and increases electro-dissolution of Al due to corrosion incentivization by chlorine species that induce pitting. This last resulted in enhancing fluoride removal and electrical energy requirements. However, NaCl optimum concentration should not be excessively increased to avoid undesired salinity in treated waters.

### 5.2. Operational Parameters

#### 5.2.1. Reactor Configuration and Operation Time

Electrocoagulation reactor could be operated in either batch or continuous flow. In a batch reactor, the electrolysis time needed for defluoridation is a crucial parameter to be evaluated since it affects kinetics, energy consumption, and therefore operating costs. Conversely, in continuous flow systems, the flow rate defines the residence time in the electrocoagulation cell [48,70].

### Batch Reactor/Electrolysis Time

Batch reactors treat a defined volume of solution that does not change over time. In a complete mixed batch reactor, the reaction rate of a constant volume of solution varies with time; so, the electrolysis time is crucial in a batch EC process [81]. An augmented fluoride removal efficiency is generally observed when increasing electrolysis time due to the sufficient production of aluminium coagulants according to Faraday's Law (Equation (22)) [70].

$$C_{Al} = \frac{I \times t \times M}{Z \times F \times V_r} \quad (22)$$

where  $C_{Al}$ ,  $I$ ,  $t$ ,  $M_{Al}$ ,  $Z$ ,  $F$  and  $V_r$  are  $Al^{3+}$  concentration ( $g\ m^{-3}$ ), current intensity (A), electrolysis time (s), the molecular weight of aluminium ( $g\ mol^{-1}$ ), number of interchanged electrons (3), Faraday constant ( $96,500\ C\ mol^{-1}$ ), the volume of the reactor ( $m^3$ ), respectively. The solution's pH can change over time to higher alkaline values due to the release of hydroxide anions from the cathodic reaction of water reduction [56]. Equation (23) describes the system energy consumption of batch systems directly dependent on electrolysis time.

$$EEC = V \times I \times t / v \quad (23)$$

where EEC,  $V$ ,  $I$ ,  $t$ ,  $v$  are the electrical energy consumption ( $Wh\ m^{-3}$ ), voltage (V), current intensity (A), electrolysis time (h), and volume of solution ( $m^3$ ), respectively [56].

According to Equation (23), the operating cost has a linear increase by progressing the electrolysis time [42,44]. Note that electrocoagulation systems should be applied till reaching the desired value of coagulant dose from the electrodisolution of sacrificial Al anodes. Additional electrolysis time over the requirements will result in unnecessary consumption of energy and excessive sludge production. Mena et al. [42] described that for a 1% increase in defluoridation, it approximately cost 2 cents for each cubic meter of water treated under experimental conditions [42].

### Continuous Reactor/Flow Rate and Retention Time

For a constant volume of a continuous reactor, an influent and effluent flow rate of solution occurs. Continuous reactors can be classified according to the mixing regime, determined by the retention time and flow rate. Emamjomeh and Sivakumar [48] indicated that the higher flow rate had a lower retention time, which affected fluoride removal due to its impact on charge loading. They also reported that the continuous reactor results in defluoridation agreed with their batch reactor results. Similar results for low retention time in a high flow rate were confirmed by Graça et al. [82]. They reported that the charge loading reduction produced lower amounts of aluminium flocs, which had an adverse impact on fluoride removal. In contrast, reduction in operation time due to the increase of flow rate decreased energy consumption.

#### 5.2.2. Electrodes

Material, inter-electrode distance, and connection types of electrodes (anode and cathode) must be considered when designing a reactor for electrocoagulation. Electrode materials determine the removal rate and the occurred chemical/electrochemical reactions for the target pollutant [56]. The inter-distance electrodes affect energy consumption and pollutant removal efficiency since ohmic resistance varies by changing this parameter [77]. The connection type of electrodes can influence the sludge formation, electrode corrosion, and most importantly, the EC process's energy consumption [83].

#### Material

For better comparative studies of electrode material, the same conditions in terms of reactor configuration and solution characteristics should be conducted. As described previously in the mechanistic section, aluminium outperforms iron-based electrodes. For instance, Un et al. [56] reported 94.2% defluoridation with a final fluoride concentration

of  $0.29 \text{ mg L}^{-1}$  with aluminum electrodes. However, under identical experimental conditions, solely 83.6% defluoridation with a final fluoride concentration of  $0.82 \text{ mg L}^{-1}$  was attained with iron electrodes. The reaction between fluoride and aluminum hydroxide  $[\text{Al}_n\text{F}_m(\text{OH})_{3n-m}]$  leads to higher removal efficacies [56].

#### Distance

The distance between anodes and cathodes affects inter-electrode resistance, influencing the defluoridation and energy consumption in an EC process [70]. For  $10 \text{ mg L}^{-1}$  initial concentration of fluoride in a batch EC reactor ( $625 \text{ A m}^{-2}$ ), the final fluoride concentration after 45 min of electrolysis decreased from 3 to  $0.8 \text{ mg L}^{-1}$  by declining the gap between electrodes from 1.5 to 0.5 cm. The lower observed efficiency at a higher distance of electrodes explained by the lower formation of coagulant due to the decreasing rate of poly-hydroxy complexes formation from the reaction between anodically formed  $\text{Al}^{3+}$  and cathodically yielded hydroxide. Hashim et al. [77] also reported that by increasing the inter-electrode distance from 0.5 to 1.1 cm, residual fluoride concentration increased from 4 to 15%. Furthermore, due to ohmic resistance variation, energy consumption augmented from 1.75 to  $3.6 \text{ kWh m}^{-3}$ . It is important to remark that very short distance between electrodes should be avoided since it decreases sludge precipitation by increasing the collision rate between the formed flocs that leads to their degradation; close distances also impede in extracting air bubbles accumulated in the system, which had an adverse impact on energy consumption [77].

#### Connection Type

Figure 5 shows the connection type of electrodes in an EC process is classified into monopolar-parallel, monopolar-serial, and bipolar connection. In a monopolar connection, each electrode separately plays as a cathode or an anode. In contrast, in a bipolar connection, the electrodes can be cathode and anode simultaneously [70,84]. Emamjomeh and Sivakumar [70] reported that the impact of the electrodes' connection on the residual fluoride concentration was insignificant, and also  $\text{Al}^{3+}/\text{F}^-$  mass ratio had no significant variation by changing connection from monopolar to bipolar. This can be explained by the fact that removal is dependent on the coagulant dose generated and not the connection mode. The amount of coagulant produced from electrodisolution is directly dependent on the current applied, as deduced from Faraday's law. However, Ghosh et al. [83] found that bipolar connection had better performance than monopolar one due to the higher surface area acted for adequate anodic oxidation.

#### 5.2.3. Electrical Characteristics

The parameters related to electrical characteristics are so of great importance in an EC process, which is classified into voltage, applied current (current intensity), current density, charge loading, and current type. Elaborating the crucial research on defluoridation case, electrical parameters will be discussed in the following paragraphs.

#### Current Type

The current type can be either direct (DC) or alternating (AC), which affects the electrode corrosion pattern, the lifetime of electrodes, the energy consumption, and the operating costs during an EC process. The formation of an impermeable layer on electrodes can reduce the EC process performance. Using AC mode would obviate this drawback by changing the current direction; so, each electrode has the anode and cathode role via current reversal [34,85]. In addition, the one direction current can reduce electrodes lifetime because of the formed impermeable layer on anodes; switching current during the AC mode affects the electrode corrosion pattern, leading to an increase in the lifetime of electrodes and a decrease in the energy consumption as well as operating costs. In the case of the current type for fluoride removal using a batch EC reactor, Ghanizadeh et al. [85] reported that the DC mode had the higher efficacy in comparison to AC mode; their

results were for the fluoride removal efficiency, but the electrode morphology and energy consumption (operating costs) for both current modes were not investigated.

### Voltage Value

Operating voltage is critical in an EC process because it determines coagulant dosage and bubble generation rate (floatation mechanism); it also affects energy consumption and mass transfer at electrodes and solution mixing. The fluoride removal efficiency enhanced with voltage enhancement in a EC reactor [85]; the applied voltage is related to other parameters, including applied current intensity, electrode connection, and inter-electrode distance. As Graça et al. [82] indicated, in three types of electrode connection, the applied voltage augmented with increasing current intensity in each one; the bipolar connection required the higher voltage than monopolar serial and parallel connection. The parallel connection indicated the lowest resistance for the division of current between electrodes. The serial connection had higher resistance due to the flow of current intensity through all electrodes, and the bipolar connection was of highest resistance since there is no inter-connection between electrodes. However, the bipolar connection indicated higher fluoride removal, the energy consumption should be considered in opting the kind of connection for defluoridation. During the continuous flow EC, the voltage remained constant, confirming that electrodes passivation was removed by flowing [82].

### Current Intensity

According to Faraday's Law (Equation (22)), the current intensity is one of the most critical parameters that can control the reaction rate; the coagulant dosage and mixing rate of an EC process are determined current intensity. Faraday's Law indicates that the proportion of I/V current concentration and electrolysis time is crucial in determining aluminium electro-dissolution [70]. Emamjomeh and Sivakumar [70] reported that defluoridation efficiency decreased in a batch reactor with declining the I/V from 683 to 273 A m<sup>-3</sup> due to the less anodic aluminium. In a continuous EC reactor with 20 L volume, Graça et al. [82] applied current intensity from 0.04 to 0.19 A and reported that the defluoridation efficiency increased in higher current intensities by releasing more aluminium during the EC process.

The definition of charge loading is critical to evaluate the process efficiency and estimate the amount of released aluminium in the different types of reactors used in the EC process.

### Charge Loading

The charge loading ( $Q_e$ ) for a batch and continuous reactors are defined as follows [86]:

$$Q_e = n \times I \times t/V \text{ (Batch reactor)} \quad (24)$$

$$Q_e = n \times I/Q \text{ (Continuous reactor)} \quad (25)$$

where  $n$  and  $Q$  are the numbers of cells, and flow rate, respectively. Hu et al. [86] indicated that similar trends in residual fluoride after both batch and continuous EC processes were observed; the residual fluoride concentration in both reactors reached under 10 mg L<sup>-1</sup> with exceeding  $Q_e = 500 \text{ C L}^{-1}$ . Govindan et al. [55] showed that increasing  $Q_e$  from 300 to 1620 C L<sup>-1</sup> enhanced the fluoride removal using both Al and Fe electrodes; they reported the 1620 C L<sup>-1</sup> charge loading for fluoride removal in a batch reactor with Al electrodes (60%) and Fe electrodes (18%).

### Current Density

Current density is another concept, which has been mostly applied to evaluate current intensity per active area of the anode during the EC process. Essadki et al. [72] confirmed that current density played a key role in the amounts of coagulant generated during the EC process. Behbahani et al. [41] and Castaneda et al. [60] reported an improvement in defluoridation with increasing current density; for initial fluoride concentration of

25 mg L<sup>-1</sup>, 94.5% fluoride removal was achieved with 111 A m<sup>-2</sup> current density (25 min), which was an optimum amount [41]. For a continuous reactor, Rosales et al. [87] indicated that residual fluoride concentration had a linear trend with flow rate at 6 A cm<sup>-2</sup>; in contrast, such trend was not observed for 4 A cm<sup>-2</sup> and 8 A cm<sup>-2</sup> due to the interferences with co-existing ions. Considering Equation (15), current density also affects energy consumption leading to an increase in operating costs. Rosales et al. [87] reported that the energy consumption increased (36.78, 93.87, 160.83 kWh m<sup>-3</sup>) by an increase in current density (4, 6, 8 mA cm<sup>-2</sup>); it was confirmed that for each current density increasing in flow rate (decrease in retention time) caused the reduction of energy consumption. The increasing trend for energy consumption and operating costs of defluoridation with current density were achieved by Changmai et al. [76].

### 5.3. Interaction of Parameters

Some research studies also evaluated the interaction effect of parameters in fluoride removal. Behbahani et al. [41] applied the response surface methodology to consider the combined effects of initial pH, initial fluoride concentration, current density, and reaction time using a batch EC process; the interaction effects between these parameters were statistically insignificant on fluoride removal efficiency. However, the interaction between current density and reaction time significantly affected the operating costs of fluoride removal. Other studies have not evaluated the interactions of parameters on fluoride removal, although these parameters might affect each other. Grich et al. [47] evaluated temperature, initial pH, conductivity, and initial fluoride concentration in different water matrices: tap and deionized water. Although they did not investigate the interaction between them directly, the increase of temperature (25 to 55 °C) facilitated the fluoride abatement related to the positive effect of temperature to the lower increase pH during the run (7.5 at 55 °C and 9 at 25 °C).

## 6. Residual Aluminium Concentration in the EC Treated Effluent

WHO [88] recommends optimization of the coagulation process in drinking water treatment plants using aluminium-based coagulants in order to minimize the residual aluminium concentration in the finished water below 0.1 and 0.2 mg L<sup>-1</sup> for large, well-operated and well-controlled plants and smaller facilities, respectively due to the potential health concerns (i.e., neurotoxicity) of aluminium. Therefore, aluminium residue present in the EC treated effluent is of great importance.

To the best of our knowledge, only a few studies exist where the residual aluminium concentration has been measured in the EC treated effluent. Mouedhen et al. [89] explored the behaviour of aluminium plate electrodes (two parallel; a specific area of electrode: 54 cm<sup>2</sup>) in electrocoagulation process using a sample synthetically prepared (1000 mg L<sup>-1</sup> Na<sub>2</sub>SO<sub>4</sub>, 100 mg L<sup>-1</sup> NaCl, 67 mg L<sup>-1</sup> Ni<sup>2+</sup>, 59 mg L<sup>-1</sup> Cu<sup>2+</sup> and 67 mg L<sup>-1</sup> Zn<sup>2+</sup>; an initial pH of 4.0). They performed an experiment to monitor the change of the dissolved aluminium concentration in the reaction solution with respect to pH evolutions during EC process run at a current density of 0.5 A dm<sup>-2</sup>. Their data indicated that the dissolved aluminium concentration continuously increased and reached a maximum of 2 mg L<sup>-1</sup> at an electrolysis time of 20 min. Meanwhile, the electrolyte pH remained quasi-constant. And then, the dissolved aluminium concentration decreased due to Al(OH)<sub>3</sub> precipitation while electrolyte pH continuously increased at the end of EC process (~80 min). Based on their results, they reported that the application of an EC process would not create any aluminium pollution.

Conversely, researches focused on defluoridation [36,52,57] revealed that a polishing step such as filtration or flocculation and settling followed the EC process was required to meet WHO permissible limit of 0.2 mg L<sup>-1</sup> for aluminium. In the study of Alimohammadi et al. [36] the residual aluminium concentrations varied between 2.85–3.28 mg L<sup>-1</sup> in the treated water at the end of the EC using hybrid Al and Fe plate electrodes (at the optimum operation conditions: an initial pH of 6, a current density of 12 mA cm<sup>-2</sup>, an

electrolysis time of 40 min, a charge loading of 0.609 Faraday  $\text{m}^{-3}$  and a flow rate of 75  $\text{mL min}^{-1}$ ).

Sinha et al. [52] investigated defluoridation by EC process using synthetically prepared sample (a mixture of NaF and NaCl in tap water). A batch EC reactor with monopolar-two plate aluminium electrodes ( $84 \times 71 \times 2.5$  mm) connection was used in their experimental study. They implemented Taguchi design method for defluoridation for the target value of fluoride in treated water as 0.7  $\text{mg L}^{-1}$ . Their data indicated that a rise in energy value produced a higher aluminium residual concentration in treated water. By applying non-linear regression analysis with the help of SYSTAT 7.0 software, they obtained the following equation to calculate the residual aluminium concentration ( $\text{Al}_R$ ) for optimum fluoride residual concentration at minimum energy value:

$$\begin{aligned} \text{Al}_R = & 0.291 - (0.734 \times F) - (0.09 \times I) + (0.242 \times t) - (0.01 \times F \times I) + (0.757 \times I \times t) \\ & - (0.322 \times F \times t) + (0.549 \times F^2) + (0.071 \times I^2) + (0.024 \times t^2) \end{aligned} \quad (26)$$

where F is the fluoride concentration in  $\text{mg L}^{-1}$ , I is the applied current in A and t is the electrolysis time in min. High residual aluminium concentrations varied between 10.72–16.82  $\text{mg L}^{-1}$  were attributed to the poor settling character of  $\text{Al}(\text{OH})_3$  flocs in the treated water. Therefore, they tested three alternative treatment applications: (i) filtration, (ii) flocculation and sedimentation followed by the filtration and (iii) bentonite added flocculation and settling followed the filtration to reduce the residual aluminium concentration in the EC treated water. Direct filtration after the EC process was insufficient and yielded high residual aluminium concentrations (7.02–13.51  $\text{mg L}^{-1}$ ) exceeding the permissible limit. Although reasonable low residual aluminium concentrations (0.27–0.40  $\text{mg L}^{-1}$ ) were obtained by the application of the flocculation and settling followed by the filtration process after EC treatment, they were slightly higher than 0.2  $\text{mg L}^{-1}$ . To enhance the efficiency of second alternative, bentonite was added to the EC treated water before flocculation application. Bentonite addition yielded extremely low residual aluminium concentrations (0.01–0.072  $\text{mg L}^{-1}$ ) and the optimum bentonite dose was determined as 2  $\text{g L}^{-1}$ .

In the view of the information mentioned above, it should be concluded that the success of the EC process on the production of safe drinking water depends not only on operation conditions such as current density, initial pH, and time but also on floc separation techniques. Therefore, selecting suitable floc separation techniques is a great important task to control and/or minimize the residual aluminium concentration in the EC treated water.

## 7. Techno-Economic Side of EC Process for Fluoride Removal

The techno-economic analysis determines the cost-effectiveness of a treatment method. In the literature, several studies have incorporated a techno-economic analysis of fluoride removal from water by electrocoagulation technology [41,42,44,48,61,62,67,77,80,83]. To summarize, there are two types of costs that need to be considered when conducting a techno-economic analysis—capital and operating costs. Capital costs are the initial cost necessary to establish the treatment method. These costs include the purchase and installation of the equipment [75]. Operating costs will be discussed later Section 7.2.

### 7.1. Energy Consumption

Energy consumption in the electrocoagulation treatment is caused by two factors—the ohmic potential within the water and between the anodes and cathodes. If there is a drop of potential in the water, increasing it between anodes and cathodes, there will be an increase in energy consumption in the system [90–92]. On the other hand, if the potential increases in the water and drops among the anodes and cathodes, energy consumption will decrease. The change in ohmic potential is caused by the presence of an electrolyte (i.e., sodium chloride) [56].

Recall that energy consumption is expressed using Equation (20). That equation states that the EC process's total energy is the accumulation of energy after each time

interval in the application. Bazrafshan et al. [38] determined that energy consumption was close to each other when using iron and aluminium electrodes for the same operating conditions. On the other hand, Takdastan et al. [93] found that the iron electrode's energy consumption was almost quadruple as high as the aluminium electrode ( $5590 \text{ kWh kg}^{-1}\text{F}^{-}$  and  $1435 \text{ kWh kg}^{-1}\text{F}^{-}$ , respectively) in the same conditions. Ün et al. [56] concluded that increasing the time to 30 min and the current density to  $3 \text{ mA cm}^2$  led to an increase in fluoride removal efficiency of up to 85.9% from water, which resulted further increase in the energy consumption of the process from 4 to  $12.5 \text{ kWh m}^{-3}$ .

### 7.2. Operating Cost

Unlike capital costs, operating costs are the costs required to upkeep the treatment method's components and ensure the EC process's daily function. Operation costs include the cost of chemicals, electrical energy, electrodes, materials, maintenance, sludge dewatering, labor, basin and pipes, disposal, and other fixed costs not listed [41,75,77]. A simplified version of the equation of operating cost has been frequently used by authors when computing the techno-economic analysis for an electrocoagulator [41]:

$$\text{OC} = aC_{\text{energy}} + bC_{\text{electrodes}} \quad (27)$$

where  $C_{\text{energy}}$  is the cost of electrical energy ( $\text{kWh m}^{-3}$ ),  $C_{\text{electrodes}}$  is the cost of electrode material ( $\text{kg Al m}^{-3}$ ). The coefficients  $a$  (price of metal) and  $b$  (cost of electricity) are different depending on the treatment location. For instance, the following coefficients were used for the cost estimation of defluoridation via the EC process. In India, Thakur and Mondal [80] suggested  $a = \$1.77 \text{ kg}^{-1} \text{ Al}$  and  $b = \$0.06 \text{ kWh}^{-1}$ . In Mexico, Castañeda et al. [60] proposed  $a = \$2.008 \text{ kg}^{-1} \text{ Al}$  and  $b = \$0.0976 \text{ kWh}^{-1}$ . In Spain, Mena et al. [42] calculated the operating cost with  $a = €1720 \text{ kg}^{-1} \text{ Al}$  and  $b = €0.117 \text{ kWh}^{-1}$ . In Iran, Behbahani et al. [41] used  $a = \$3 \text{ kg}^{-1} \text{ Al}$  and  $b = \$0.0128 \text{ kWh}^{-1}$ .

Energy and electrode costs are derived from the following equation [83]:

$$C_{\text{energy}} = U \times I \times t_{\text{EC}} / V \quad (28)$$

Electrode costs are calculated from Faraday's Law [83], as shown in Equation (22):

### 7.3. Optimization (Costs to Defluoridation Water by EC)

The costs to defluoridate water by EC have been estimated in the recent scientific literature. Bhagawan et al. [94] concluded that the total cost could range from 0.28 to  $0.98 \text{ \$ m}^{-3}$  of treated water. Besides, the type of sacrificial electrode and electrode configuration can affect the cost of EC. For example, Khan et al. [95] remarked that evaluating the two electrode materials, aluminium and iron, aluminium was better in terms of cost-effectiveness when the EC process is performed in batch operation mode. Ghosh et al. [83] calculated the monopolar configuration costs as 0.075 to  $0.12 \text{ \$ m}^{-3}$  for the electrodes and 0.07 to  $0.19 \text{ \$ m}^{-3}$  for the cost of energy. Electrode and energy costs for bipolar configuration were 0.15 to  $0.38 \text{ m}^{-3}$  and 0.09 to  $0.24 \text{ \$ m}^{-3}$  respectively. Behbahani et al. [41] reported that peak operating costs were related to the current density and reaction time. The maximum current yielded a cost of  $1.48 \text{ \$ m}^{-3}$ , while the longest reaction time leads to a cost of  $1.27 \text{ \$ m}^3$  [41]. Hashim et al. [77] computed that the operating costs for defluoridation drinking water using EC was  $0.379 \text{ \$ m}^{-3}$ . Emamjomeh and Sivakumar [48] estimated a cost between  $0.25 \text{ \$ m}^{-3}$  and  $0.45 \text{ \$ m}^{-3}$ . On the other hand, Thakur and Mondal [80] found operating costs to be  $0.343 \text{ \$ m}^{-3}$ . It is also imperative to know that these costs vary based on the initial fluoride concentration. An increase in fluoride concentration will increase the cost of electrodes and the cost of energy. Also, the desired removal efficiency is important when considering the cost of EC treatment of pollutants.

Overall, the defluoridation by EC process can be cost-effective in comparison with other methods. The EC process does not have the chemical cost requirement as other treatment processes, such as chemical coagulation. Therefore, it can be considered eco-friendly.

However, EC may have a higher maintenance cost. In brief, the operational costs fluctuate between 0.075–1.48 USD m<sup>-3</sup>. These values depend on the type of reactor, electrode material, operating conditions, and water characteristics. Compared to other techniques such as sorption, precipitation, and membrane, EC is a medium relative economic cost process [96]. Lacson et al. [96] analyzed several studies related to removing of fluoride from water through different technologies.

Moreover, they extrapolated and estimated the operational costs of such technologies. On the one hand, the sorption techniques are the most expensive process to treat fluoride-containing water (around ten to twenty times that other processes, ~0.47 € m<sup>-3</sup>) followed by reverse osmosis membrane technique (~0.32 € m<sup>-3</sup>). On the other hand, the coagulation-flocculation process is the cheapest process (~0.2 € m<sup>-3</sup>) to remove fluoride from contaminated water. They concluded that electro-based techniques represent a low-cost alternative to reduce high concentrations of fluoride in water.

Also, the disposal of sludge could be expensive depending on the fluoride to be treated and the EC reactor's operating conditions [97]. A potential option to be considered is to reuse the sludge for other applications. However, reuse is contingent on the physical properties of the sludge and its impacts on the environment. If reuse requires high capital, it may not be the best option [97].

## 8. Scaling-Up of EC Defluoridation Plants in Regions around the World

Scaling-up of the EC system is a fundamental step to transfer laboratory-scale processes to industrial-scale. One of the most important challenges of the EC process in removing fluoride from water is the lack of attention to its industrial scaling-up since most of the research done in this field is on the laboratory-scale and just a few of them on the pilot-scale. A summary of important recent efforts is mentioned here.

Mena et al. [42] reported batch and continuous lab-scale (volume of 2 L) EC for fluoride removal from underground volcanic water. They found that the highest removal efficiency was obtained at the optimum current density of 5 mA cm<sup>-2</sup> in batch operation mode. Under the optimal condition of the residence time (10 min) and distance between the electrodes (0.5 cm) in the continuous-flow operation, the applied current density varied on the raw water's initial fluoride concentration. An advanced scale-up design proposed by Betancor-Abreu et al. [74] examined the defluoridation from volcanic springs ground waters in the island of Tenerife (Spain) with average initial fluoride concentrations above 7 mg L<sup>-1</sup>. They used different EC reactors involving the capacity of 145, 368, and 2000 mL. The process efficacy was confirmed under optimal operating conditions by reducing the fluoride concentration from 7.35 to 1.4 mg L<sup>-1</sup>. Emamjomeh and Sivakumar [70] set up a bench-scale EC batch reactor with a working volume of 3.66 L. The results confirmed that the EC is a viable process for the defluoridation of water. In another study, Emamjomeh and Sivakumar [48] assessed the water defluoridation using a continuous flow pilot-scale EC reactor containing 7.9 L net volume. They inferred that the maximum fluoride removal efficiency was reached when the highest current density was employed.

Rosales et al. [87] constructed a pre-pilot scale EC reactor that involved 13 parallel aluminum plates located in a tank of 20 L capacity for groundwater sample, which gathered from a deep well situated in the northeastern region of Guanajuato, Mexico. They revealed that fluoride concentrations after the EC process (0.19 mg L<sup>-1</sup>) meet the WHO guidelines. Another pre-pilot setup was performed to treat groundwater with an initial fluoride concentration of 5.5 mg L<sup>-1</sup> by EC unit in a continuous filter press reactor containing a three-cell stack equipped with aluminum electrodes. The authors proved that the EC reactor under operating parameters of the current density of 5–7 mA cm<sup>-2</sup> and flow rate of 0.23–0.93 cm s<sup>-1</sup> reached fluoride removal efficiencies, which met the acceptable WHO standard permissible limit. The optimal energy consumption of 6.7 kWh m<sup>-3</sup> was achieved at 6 mA cm<sup>-2</sup> current density and a 0.23 cm s<sup>-1</sup> flow rate [98]. Castañeda et al. [60] successfully applied an EC up-flow reactor with 7 parallel aluminum electrodes placed horizontally, making up a six-cell stack that contained a 15 L-capacity for a groundwater

sample with an initial fluoride concentration of  $4.08 \text{ mg L}^{-1}$ . The well-engineered EC reactor results showed that the final concentration of fluoride fulfilled the WHO guideline at a proper operational cost of  $0.441 \text{ USD m}^{-3}$ . A continuous lab-scale EC reactor with 5 L of capacity was tested using 4 aluminium electrodes for water containing a concentration of  $15 \text{ mg F}^{-1} \text{ L}^{-1}$  by Graça et al. [82]. In that work, they found that the EC process removed 97% of fluoride ions. Besides, the proposed reactor's efficiency for treating higher volumes of contaminated water through a volume of 20 L on a pre-pilot scale was evaluated. Complete abatement of fluoride was observed with an energy consumption of  $506 \text{ kWh m}^{-3}$ .

A comparison between a lab and full scale was undertaken by Gwala et al. [99] to remove fluoride from raw water containing an initial concentration of  $4.8 \text{ mg L}^{-1}$ . On a lab-scale of 5 L capacity, they used three aluminium plate electrodes in a monopolar configuration. The results at optimal laboratory conditions (pH 6.5, current intensity 2 A, and residence time of 20 min) showed that the fluoride's residual concentration reached  $0.94 \text{ mg L}^{-1}$ . On the other hand, the final fluoride concentration was reduced to  $0.89 \text{ mg L}^{-1}$  in the aforementioned optimal conditions, only by changing the treatment time and current intensity to 60 min and 20 A, respectively, in a full-scale EC defluoridation plant of 600 L, which was operated at Dongargaon, India. In conclusion, the residual fluoride concentration was quasi-identical in both lab and full-scale EC reactors. Moreover, the permissible limit for fluoride was reached according to the Indian standard for drinking water.

Bhagawan et al. [94] examined a lab-scale cylindrical reactor with a working volume of 2.5 L operating under semi-continuous flow-EC using aluminum and iron electrodes and stainless steel as anodes and cathodes, respectively. The application of the novel semi-continuous flow EC reactor demonstrated that the fluoride concentration of  $8 \text{ mg L}^{-1}$  in groundwater met the WHO drinking limits under conditions of 30 min,  $300 \text{ mL min}^{-1}$  flow rate, 15 V applied voltage, and pH 7. López-Guzmán et al. [10] investigated the EC lab-scale reactor for well water treatment containing  $4.18 \text{ mg L}^{-1}$  fluoride from the Guadiana Valley, Mexico. The combination of aluminium and iron as electrode materials within the EC reactor comprising 1.5 L effective volume was used. The EC tests revealed that under optimal conditions (current density of  $4.5 \text{ mA cm}^{-2}$ , initial pH of 5, and treatment time of 15 min), fluoride removal with an initial concentration of  $5 \text{ mg L}^{-1}$  reached 85.68%, which adhered to drinking water limits of the WHO and Mexican regulations. In addition, the fluoride removal rate enhanced to 94.98% in acidic conditions. Silva et al. [66] proposed a lab-scale EC acrylic tank with a 3 L capacity and aluminium electrodes embedded in it for fluoride abatement from contaminated drinking water. They observed that virtually complete removal of fluoride could be achieved after 30 min of the EC process. The study was carried out by Al-EC reactor from water wells in the states of San Luis Potosi and Aguascalientes in central Mexico, showed that a snap reduction from  $5.17$  to  $1.5 \text{ mg L}^{-1}$  (~71% removal efficiency) fluoride concentration was achieved only in 4 min [100].

Among all the efforts in developing the EC process for defluoridation from tap water or groundwater, only one work attempted to study the industrial scaling-up. However, these studies might evoke a clear path for applying this process on a larger scale. Further systematic studies must be performed in a continuous flow mode to scale-up this to establish the EC as a cost-effective, robust, and reliable technology for fluoride removal. According to the literature survey, there is sufficient information on scaling-up the defluoridation-EC process from laboratory to industrial scale or even to pilot plant scale. Therefore, the application of the combined EC process with other treatment processes might improve its performance. Furthermore, larger scale and long-term pilot studies are required under different operating conditions for defluoridation of drinking water or groundwater.

## 9. Integrated EC Processes for Fluoride Removal

Electrocoagulation, as a method of defluoridation, especially for drinking water, has received significant interest in the last 30 years. Although the EC process can be successfully used to treat drinking water of low initial fluoride concentrations, sometimes it may fail to

meet the drinking water standards. For this reason, several researchers are moving toward combined EC processes to increase pollutants removal efficiency, such as fluoride found in drinking water. EC process can be used as a pre- or post-polishing process depending on the type of contaminants present in water [101–105].

### 9.1. Combined EC and Adsorption Treatment System

Wali and Saidutta [101] applied a combined EC–adsorption treatment process to remove fluoride from drinking water. Batch experiments were performed using aluminium anodes and stainless-steel cathodes connected in monopolar and bipolar arrangements with NaCl as supporting electrolyte. After the EC treatment step, two adsorbents, namely tri-calcium phosphate  $\text{Ca}_3(\text{PO}_4)_2$  and activated alumina, were tested to remove the residual fluoride in the EC-treated water. They reported that using NaCl as a supporting electrolyte ( $200 \text{ NaCl mg L}^{-1}$ ), the fluoride removal efficiencies were 83%, 93.46%, and 95% for EC alone, EC-adsorption with tri tricalcium phosphate processes, and EC-adsorption with activated alumina, respectively. The second contribution to the application of EC–adsorption processes was performed by Jalil et al. [102]. They used aluminium plates as anode and cathode and activated carbon as an adsorbent. They assessed the effects of the applied voltage (5, 15, and 20 V) and the adsorbent dose (0.2, 0.5, and 1 g) on the fluoride removal efficiency using a synthetically prepared fluoride solution (initial concentration  $100 \text{ mg L}^{-1}$ ). The overall performance significantly improved in the combined processes compared to both electrocoagulation and adsorption alone. The fluoride removal efficiencies were 41.1%, 2.86%, and 67.25% using electrocoagulation, adsorption, and combined process, respectively. These results justified using a combined EC-AD process instead of a single treatment process to achieve a higher quality of the treated sample and demonstrated synergy between the two processes.

### 9.2. Combined EC and Precipitation or Chemical Coagulation Treatment System

The first contribution that used combined chemical coagulation with EC treatment was proposed by Zhao et al. [103] to remove fluoride from drinking water using ultra-pure Al electrodes and  $\text{AlCl}_3$  as a coagulant. They compared the performance of the combined process and the acid-adding EC process. They reported that when  $\text{Al}^{+3}$  dosages were more than 1.5 mM, fluoride removal was more than 90% for both processes. However, the combined process was characterized by a little energy consumption, which was only one-third consumed in the acid-adding EC process. Besides, Al consumption of the sacrificial electrode decreased in the case of the chemical-electrical coagulation. These results confirmed that a combined treatment has promising application prospects. Another contribution of using EC-assisted chemical coagulation was performed by Kashi et al. [104]. They used an EC cell with copper electrodes and poly aluminium chloride (PAC) as a chemical coagulant. The fluoride removal efficiencies were determined as 87 and 99% for EC and EC combined with PAC, respectively at optimum conditions (a distance between electrodes of 1.5 cm, a current density of  $4.5 \text{ mA cm}^{-2}$ , a contact time of 10 m, and a pH of 7.5).

An interesting study focused on the removal of fluoride ions from drinking water by flocculation-assisted EC was published by Sandoval et al. [59]. A continuous filter press EC reactor using aluminum electrodes, which was coupled to a flocculator and clarifier was designed in their study, as shown in Figure 6. Synthetically prepared drinking water sample ( $10 \text{ mg F L}^{-1}$  dissolved in  $0.5 \text{ g L}^{-1}$ ,  $\text{Na}_2\text{SO}_4$  and  $1.5 \text{ mg L}^{-1} \text{ ClO}^-$  at pH 7.7 and conductivity  $410 \text{ }\mu\text{S cm}^{-1}$ ) was used in their experiments. A current density of  $5 \text{ mA cm}^{-2}$  and an average linear flow velocity  $1.82 \text{ cm s}^{-1}$  were applied to reduce the fluoride concentration from 10 to  $1 \text{ mg L}^{-1}$ , resulted in the best energy consumption of  $0.37 \text{ kW h m}^{-3}$ . They reported that the proposed combined treatment system could serve as a starting point to remove fluoride from real groundwater.

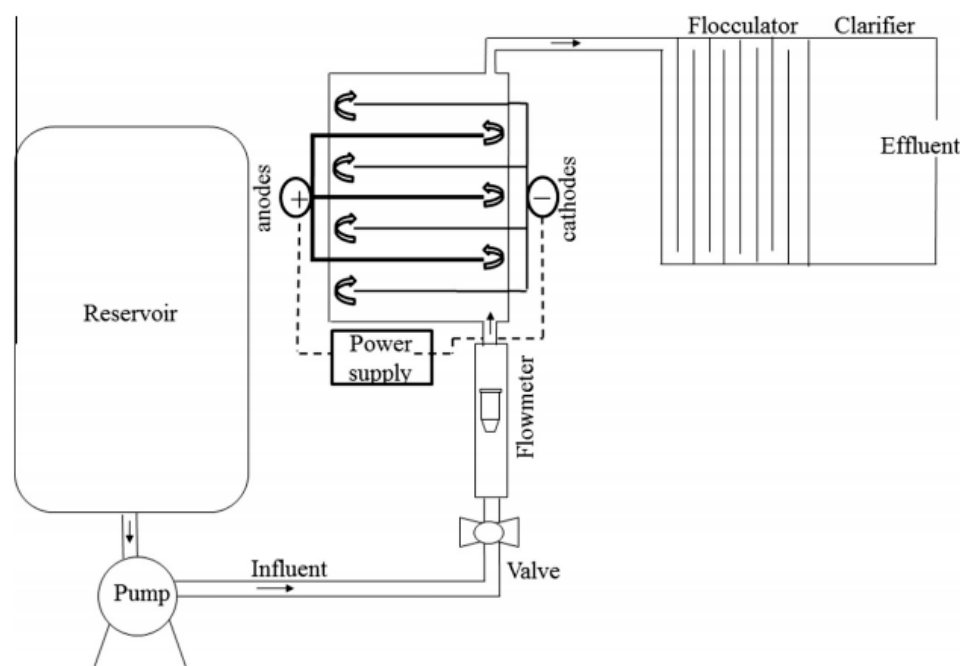


**Figure 6.** The filter press reactor coupled to a flocculator and clarifier (reprinted from [59] with permission from Elsevier).

### 9.3. Combined Electrocoagulation/Electro Flotation (EC/EF) Treatment Systems

It is well known that the electrocoagulation process produces hydrogen gas from the reduction of water molecules at the cathode. The hydrogen gas bubbles help in the floating part of the produced lumps of the coagulated pollutants formed in the electrochemical cell. The electroflotation (EF) of the coagulated sludge is enhanced using a suitable reactor design or adding extra floating gas if the produced gas in the cell is insufficient to complete the flotation process.

The first contribution in this EC/EF treatment process was reported by Zuo et al. [57]. The researchers applied a combined EC/EF process using an experimental apparatus consisted of three different chambers, as shown in Figure 7. Chamber 1 was designed for the EC process with Al electrodes, chamber 2 was used to enhance flocculation, and chamber 3 was employed for the EF process with two-rod anodes (Ti/IrO<sub>2</sub>-SnO<sub>2</sub>-Sb<sub>2</sub>O<sub>5</sub>) and three rods of Ti cathodes. The volume of these chambers was 0.4, 0.5, and 0.85 L, respectively. The fluoride ion concentration was reduced from 4.0 to 0.87 mg L<sup>-1</sup> at 200 s cm<sup>-1</sup> conductivity, 22 A m<sup>-2</sup> current density, and an average current density EF step of 75 A m<sup>-2</sup>. They concluded that the combined EC/EF process is an efficient fluoride removal process from drinking water.

Essadki et al. [105] designed two EC cells consisting of a stirred tank reactor (STR) and an airlift reactor (ALR) to remove fluoride from drinking water as shown in Figure 8. Flat aluminium electrodes were utilized as anodes and cathodes in both cells. The ALR was a new design of such reactors applied for the electrocoagulation/electroflotation process. In addition, its operation and geometrical configuration were different from conventional airlift reactors since there was no gas phase being sparged at the bottom of the riser. In their system, the overall liquid recirculation was provided by the density difference between the fluids in the riser and the downcomer consequence of production of hydrogen gas microbubbles on the cathode.



## 10. Conclusions and Outlook

The present review has been devoted to exploring the applicability of the electrocoagulation method to remove fluoride from drinking water. This work consists of a comprehensive review for the removal of fluoride using the EC technology as it discussed all the aspects of the process, including the effects of the operating parameters (such as the pH of the solution, electrodes gapping, and current density), the chemistry of solutions, design of the EC reactor, characteristics of flow, the configuration of electrodes, and the type of the electrical current on the removability of fluoride from solutions. Additionally, the electrochemical reactions and removal paths of pollutants, operating cost, scaling of the EC reactors, hybridization of the EC process with other technologies, and other EC method applications were presented and discussed. Furthermore, the main limitations, advantages, and disadvantages of the EC method were carefully addressed. It is confirmed that the EC method could be considered an efficient, eco-friendly, and economically effective method for fluoride removal from drinking water. Simultaneously, to ensure the EC reactors' efficient performance, the critical operating parameters must be optimized. Such is the case of EC reactors fitted with parallel plate electrodes (in continuous mode of operation). This type of reactors offers an optimal functioning during the EC process because of the dispersion between the solution and the coagulating species. Moreover, the current distribution is uniform. Also, considering the scaling, these reactors are easier to achieve this goal.

Further fluoride removal studies by electrocoagulation should be coupled with rigorous computational fluids dynamic simulations (flocs formation, gas bubbles generation) to design optimal new electrochemical reactors to increase the fluoride removal efficiency under lower energy requirements. Additionally, the electrodes' material must be carefully selected according to the properties of the targeted pollutants. It is highly recommended for future work to carry out more studies about the generated sludge's recyclability in the construction industry. This type of sludge contains a considerable amount of electrodes' material (usually aluminium or iron) that could be activated and used in concrete production.

**Author Contributions:** Conceptualization, M.M.; literature search, designing of figures and tables, writing—original draft preparation, S.M.A., I.K., E.K.N., Z.A.Q., Z.N., A.E.D.M., M.A.S. and E.B.; validation and supervision, M.M.E.; writing—review and editing, M.M., Z.F., I.K. and M.M.E.; provided comments and proof-read, I.K., Z.F., M.A.S. All authors have read and agreed to the published version of the manuscript.

**Funding:** This research received no external funding.

**Institutional Review Board Statement:** This study did not involve humans or animals.

**Informed Consent Statement:** This study did not involve humans.

**Data Availability Statement:** This study did not report any data.

**Acknowledgments:** The support of the Research Vice-Chancellor of Qazvin University of Medical Sciences (IR.QUMS.REC.1399.472) is wholeheartedly appreciated. Milad Mousazadeh gratitudes the Iran's National Elites Foundation (INEF) for granting the Elite Soldier Award, No. 15/11529. Miguel A. Sandoval is grateful to Consejo Nacional de Ciencia y Tecnología, Mexico (CONACYT) for granting the postdoctoral scholarship, No. 386022. A.E.D Mahmoud would like to thank "Green Technology Group".

**Conflicts of Interest:** The authors declare no conflict of interest.

## References

1. Yadav, K.K.; Kumar, S.; Pham, Q.B.; Gupta, N.; Rezania, S.; Kamyab, H.; Yadav, S.; Vymazal, J.; Kumar, V.; Tri, D.Q. Fluoride contamination, health problems and remediation methods in Asian groundwater: A comprehensive review. *Ecotoxicol. Environ. Saf.* **2019**, *182*, 109362. [[CrossRef](#)]

2. Rasool, A.; Farooqi, A.; Xiao, T.; Ali, W.; Noor, S.; Abiola, O.; Ali, S.; Nasim, W. A review of global outlook on fluoride contamination in groundwater with prominence on the Pakistan current situation. *Environ. Geochem. Health* **2018**, *40*, 1265–1281. [[CrossRef](#)]
3. Alkurdi, S.S.; Al-Juboori, R.A.; Bundschuh, J.; Hamawand, I. Bone char as a green sorbent for removing health threatening fluoride from drinking water. *Environ. Int.* **2019**, *127*, 704–719. [[CrossRef](#)]
4. Ali, S.; Thakur, S.K.; Sarkar, A.; Shekhar, S. Worldwide contamination of water by fluoride. *Environ. Chem. Lett.* **2016**, *14*, 291–315. [[CrossRef](#)]
5. WHO. *Guidelines for Drinking-Water Quality: Recommendations (Vol. 1)*; World Health Organization: Geneva, Switzerland, 2004; Available online: <https://apps.who.int/iris/handle/10665/42852> (accessed on 15 February 2021).
6. Petrone, P.; Guarino, F.M.; Giustino, S.; Gombos, F. Ancient and recent evidence of endemic fluorosis in the Naples area. *J. Geochem. Explor.* **2013**, *131*, 14–27. [[CrossRef](#)]
7. Kagne, S.; Jagtap, S.; Dhawade, P.; Kamble, S.; Devotta, S.; Rayalu, S. Hydrated cement: A promising adsorbent for the removal of fluoride from aqueous solution. *J. Hazard. Mater.* **2008**, *154*, 88–95. [[CrossRef](#)]
8. Alabdulaaly, A.I.; Al-Zarah, A.I.; Khan, M.A. Occurrence of fluoride in ground waters of Saudi Arabia. *Appl. Water Sci.* **2013**, *3*, 589–595. [[CrossRef](#)]
9. Yuan, L.; Fei, W.; Jia, F.; Jun-Ping, L.; Qi, L.; Fang-Ru, N.; Xu-Dong, L.; Shu-Lian, X. Health risk in children to fluoride exposure in a typical endemic fluorosis area on Loess Plateau, north China, in the last decade. *Chemosphere* **2020**, *243*, 125451. [[CrossRef](#)] [[PubMed](#)]
10. López-Guzmán, M.; Alarcón-Herrera, M.; Irigoyen-Campuzano, J.; Torres-Castañón, L.; Reynoso-Cuevas, L. Simultaneous removal of fluoride and arsenic from well water by electrocoagulation. *Sci. Total Environ.* **2019**, *678*, 181–187. [[CrossRef](#)]
11. Loganathan, P.; Vigneswaran, S.; Kandasamy, J.; Naidu, R. Defluoridation of drinking water using adsorption processes. *J. Hazard. Mater.* **2013**, *248*, 1–19. [[CrossRef](#)]
12. Mourabet, M.; El Rhilassi, A.; El Boujaady, H.; Bennani-Ziatni, M.; El Hamri, R.; Taitai, A. Removal of fluoride from aqueous solution by adsorption on hydroxyapatite (HAp) using response surface methodology. *J. Saudi Chem. Soc.* **2015**, *19*, 603–615. [[CrossRef](#)]
13. Wang, Y.; Chen, N.; Wei, W.; Cui, J.; Wei, Z. Enhanced adsorption of fluoride from aqueous solution onto nanosized hydroxyapatite by low-molecular-weight organic acids. *Desalination* **2011**, *276*, 161–168. [[CrossRef](#)]
14. Huang, H.; Liu, J.; Zhang, P.; Zhang, D.; Gao, F. Investigation on the simultaneous removal of fluoride, ammonia nitrogen and phosphate from semiconductor wastewater using chemical precipitation. *Chem. Eng. J.* **2017**, *307*, 696–706. [[CrossRef](#)]
15. Wang, L.; Zhang, Y.; Sun, N.; Sun, W.; Hu, Y.; Tang, H. Precipitation Methods Using Calcium-Containing Ores for Fluoride Removal in Wastewater. *Minerals* **2019**, *9*, 511. [[CrossRef](#)]
16. Akafu, T.; Chimdi, A.; Gomoro, K. Removal of Fluoride from Drinking Water by Sorption Using Diatomite Modified with Aluminum Hydroxide. *J. Anal. Methods Chem.* **2019**, *2019*. [[CrossRef](#)] [[PubMed](#)]
17. Tripathy, S.S.; Bersillon, J.-L.; Gopal, K. Removal of fluoride from drinking water by adsorption onto alum-impregnated activated alumina. *Sep. Purif. Technol.* **2006**, *50*, 310–317. [[CrossRef](#)]
18. Meenakshi, S.; Viswanathan, N. Identification of selective ion-exchange resin for fluoride sorption. *J. Colloid Interface Sci.* **2007**, *308*, 438–450. [[CrossRef](#)]
19. Onyango, M.S.; Kojima, Y.; Aoyi, O.; Bernardo, E.C.; Matsuda, H. Adsorption equilibrium modeling and solution chemistry dependence of fluoride removal from water by trivalent-cation-exchanged zeolite F-9. *J. Colloid Interface Sci.* **2004**, *279*, 341–350. [[CrossRef](#)] [[PubMed](#)]
20. Amor, Z.; Bariou, B.; Mameri, N.; Taky, M.; Nicolas, S.; Elmidaoui, A. Fluoride removal from brackish water by electro dialysis. *Desalination* **2001**, *133*, 215–223. [[CrossRef](#)]
21. Arahman, N.; Mulyati, S.; Lubis, M.R.; Takagi, R.; Matsuyama, H. The removal of fluoride from water based on applied current and membrane types in electro dialysis. *J. Fluor. Chem.* **2016**, *191*, 97–102. [[CrossRef](#)]
22. Sharma, P.P.; Yadav, V.; Maru, P.D.; Makwana, B.S.; Sharma, S.; Kulshrestha, V. Mitigation of fluoride from brackish water via electro dialysis: An environmentally friendly process. *ChemistrySelect* **2018**, *3*, 779–784. [[CrossRef](#)]
23. Cui, H.; Qian, Y.; An, H.; Sun, C.; Zhai, J.; Li, Q. Electrochemical removal of fluoride from water by PAOA-modified carbon felt electrodes in a continuous flow reactor. *Water Res.* **2012**, *46*, 3943–3950. [[CrossRef](#)]
24. Zhao, X.; Zhang, B.; Liu, H.; Qu, J. Simultaneous removal of arsenite and fluoride via an integrated electro-oxidation and electrocoagulation process. *Chemosphere* **2011**, *83*, 726–729. [[CrossRef](#)] [[PubMed](#)]
25. Abdulhadi, B.; Kot, P.; Hashim, K.; Shaw, A.; Muradov, M.; Al-Khaddar, R. Continuous-flow electrocoagulation (EC) process for iron removal from water: Experimental, statistical and economic study. *Sci. Total Environ.* **2020**, 143417. [[CrossRef](#)] [[PubMed](#)]
26. Hashim, K.S.; AlKhaddar, R.; Shaw, A.; Kot, P.; Al-Jumeily, D.; Alwash, R.; Aljefery, M.H. Electrocoagulation as an eco-friendly River water treatment method. In *Advances in Water Resources Engineering and Management*; Springer: Singapore, 2020; pp. 219–235. [[CrossRef](#)]
27. Tahreen, A.; Jami, M.S.; Ali, F. Role of electrocoagulation in wastewater treatment: A developmental review. *J. Water Process Eng.* **2020**, *37*, 101440. [[CrossRef](#)]
28. Moussa, D.T.; El-Naas, M.H.; Nasser, M.; Al-Marri, M.J. A comprehensive review of electrocoagulation for water treatment: Potentials and challenges. *J. Environ. Manag.* **2017**, *186*, 24–41. [[CrossRef](#)]

29. Yasri, N.; Hu, J.; Kibria, M.G.; Roberts, E.P.L. Electrocoagulation Separation Processes. In *Multidisciplinary Advances in Efficient Separation Processes*; American Chemical Society: Washington, DC, USA, 2020; Volume 1348, pp. 167–203. [[CrossRef](#)]
30. Kabdaşlı, I.; Arslan-Alaton, I.; Ölmez-Hancı, T.; Tünay, O. Electrocoagulation applications for industrial wastewaters: A critical review. *Environ. Technol. Rev.* **2012**, *1*, 2–45. [[CrossRef](#)]
31. Garcia-Segura, S.; Eiband, M.M.S.G.; de Melo, J.V.; Martínez-Huitle, C.A. Electrocoagulation and advanced electrocoagulation processes: A general review about the fundamentals, emerging applications and its association with other technologies. *J. Electroanal. Chem.* **2017**, *801*, 267–299. [[CrossRef](#)]
32. Liu, H.; Zhao, X.; Qu, J. Electrocoagulation in water treatment. In *Electrochemistry for the Environment*; Springer: Singapore, 2010; pp. 245–262. [[CrossRef](#)]
33. Mao, X.; Hong, S.; Zhu, H.; Lin, H.; Wei, L.; Gan, F. Alternating pulse current in electrocoagulation for wastewater treatment to prevent the passivation of Al electrode. *J. Wuhan Univ. Technol. Mater. Sci. Ed.* **2008**, *23*, 239–241. [[CrossRef](#)]
34. Karamati-Niaragh, E.; Moghaddam, M.R.A.; Emamjomeh, M.M.; Nazlabadi, E. Evaluation of direct and alternating current on nitrate removal using a continuous electrocoagulation process: Economical and environmental approaches through RSM. *J. Environ. Manag.* **2019**, *230*, 245–254. [[CrossRef](#)]
35. Elshawi, E.S.; Ruda, H.E.; Dawson, F.P. Principles and Design of an Integrated Magnetics Structure for Electrochemical Applications. *IEEE Trans. Ind. Appl.* **2020**. [[CrossRef](#)]
36. Alimohammadi, M.; Mesdaghinia, A.; Shayesteh, M.; Mansoorian, H.; Khanjani, N. The efficiency of the electrocoagulation process in reducing fluoride: Application of inductive alternating current and polarity inverter. *Int. J. Environ. Sci. Technol.* **2019**, *16*, 8239–8254. [[CrossRef](#)]
37. Amarasooriya, A.; Kawakami, T. Electrolysis removal of fluoride by magnesium ion-assisted sacrificial iron electrode and the effect of coexisting ions. *J. Environ. Chem. Eng.* **2019**, *7*, 103084. [[CrossRef](#)]
38. Bazrafshan, E.; Ownagh, K.A.; Mahvi, A.H. Application of electrocoagulation process using iron and aluminum electrodes for fluoride removal from aqueous environment. *J. Chem.* **2012**, *9*, 2297–2308. [[CrossRef](#)]
39. Kabdasli, I.; Konuk, K.; Tunay, O. Defluoridation of drinking water by electrocoagulation with stainless steel electrodes. *Fresenius Environ. Bull.* **2017**, *26*, 345–351.
40. Ün, Ü.T.; Koparal, A.S.; Ögütveren, Ü.B.; Durucan, A. Electrochemical process for the treatment of drinking water. *Fresenius Environ. Bull.* **2010**, *19*, 1906–1910.
41. Behbahani, M.; Moghaddam, M.A.; Arami, M. Techno-economical evaluation of fluoride removal by electrocoagulation process: Optimization through response surface methodology. *Desalination* **2011**, *271*, 209–218. [[CrossRef](#)]
42. Mena, V.; Betancor-Abreu, A.; González, S.; Delgado, S.; Souto, R.; Santana, J. Fluoride removal from natural volcanic underground water by an electrocoagulation process: Parametric and cost evaluations. *J. Environ. Manag.* **2019**, *246*, 472–483. [[CrossRef](#)]
43. Rebhun, M.; Lurie, M. Control of organic matter by coagulation and floc separation. *Water Sci. Technol.* **1993**, *27*, 1–20. [[CrossRef](#)]
44. Thakur, L.S.; Mondal, P. Simultaneous arsenic and fluoride removal from synthetic and real groundwater by electrocoagulation process: Parametric and cost evaluation. *J. Environ. Manag.* **2017**, *190*, 102–112. [[CrossRef](#)]
45. Wang, X.; Xu, H.; Wang, D. Mechanism of fluoride removal by AlCl<sub>3</sub> and Al<sub>13</sub>: The role of aluminum speciation. *J. Hazard. Mater.* **2020**, 122987. [[CrossRef](#)]
46. Emamjomeh, M.M.; Sivakumar, M.; Varyani, A.S. Analysis and the understanding of fluoride removal mechanisms by an electrocoagulation/flotation (ECF) process. *Desalination* **2011**, *275*, 102–106. [[CrossRef](#)]
47. Grich, N.B.; Attour, A.; Mostefa, M.L.P.; Guesmi, S.; Tlili, M.; Lopicque, F. Fluoride removal from water by electrocoagulation: Effect of the type of water and the experimental parameters. *Electrochim. Acta* **2019**, *316*, 257–265. [[CrossRef](#)]
48. Emamjomeh, M.M.; Sivakumar, M. Fluoride removal by a continuous flow electrocoagulation reactor. *J. Environ. Manag.* **2009**, *90*, 1204–1212. [[CrossRef](#)]
49. Kim, K.-J.; Baek, K.; Ji, S.; Cheong, Y.; Yim, G.; Jang, A. Study on electrocoagulation parameters (current density, pH, and electrode distance) for removal of fluoride from groundwater. *Environ. Earth Sci.* **2016**, *75*, 45. [[CrossRef](#)]
50. Zhu, J.; Zhao, H.; Ni, J. Fluoride distribution in electrocoagulation defluoridation process. *Sep. Purif. Technol.* **2007**, *56*, 184–191. [[CrossRef](#)]
51. Taşbatan, M.; Tünay, O.; Kabdaşlı, N.I.; Ölmez\_Hancı, T. Fluoride Removal By Electrocoagulation Process Using Aluminium Electrodes At Acidic pH Range. *J. Selçuk Univ. Nat. Appl. Sci.* **2013**, *1*, 769–779.
52. Sinha, R.; Mathur, S.; Brighu, U. Aluminium removal from water after defluoridation with the electrocoagulation process. *Environ. Technol.* **2015**, *36*, 2724–2731. [[CrossRef](#)]
53. Ya, V.; Chen, Y.-C.; Chou, Y.-H.; Choo, K.-H.; Liu, J.-C.; Ma Montero-Ocampo, C.; Villafañe, J.M. Effect of dissolved species on the fluoride electro-removal from groundwater. *ECS Trans.* **2010**, *28*, 57. [[CrossRef](#)]
54. Ya, V.; Chen, Y.-C.; Chou, Y.-H.; Choo, K.-H.; Liu, J.-C.; Mameda, N.; Li, C.-W. Cryolite (Na<sub>3</sub>AlF<sub>6</sub>) crystallization for fluoride recovery using an electrolytic process equipped with a sacrificial aluminum anode. *J. Hazard. Mater.* **2019**, *368*, 90–96. [[CrossRef](#)]
55. Govindan, K.; Raja, M.; Maheshwari, S.U.; Noel, M.; Oren, Y. Comparison and understanding of fluoride removal mechanism in Ca<sup>2+</sup>, Mg<sup>2+</sup> and Al<sup>3+</sup> ion assisted electrocoagulation process using Fe and Al electrodes. *J. Environ. Chem. Eng.* **2015**, *3*, 1784–1793. [[CrossRef](#)]
56. Ün, Ü.T.; Koparal, A.S.; Oğutveren, U.B. Fluoride removal from water and wastewater with a batch cylindrical electrode using electrocoagulation. *Chem. Eng. J.* **2013**, *223*, 110–115. [[CrossRef](#)]

57. Zuo, Q.; Chen, X.; Li, W.; Chen, G. Combined electrocoagulation and electroflotation for removal of fluoride from drinking water. *J. Hazard. Mater.* **2008**, *159*, 452–457. [[CrossRef](#)]
58. Das, D.; Nandi, B.K. Simultaneous removal of fluoride and Fe (II) ions from drinking water by electrocoagulation. *J. Environ. Chem. Eng.* **2020**, *8*, 103643. [[CrossRef](#)]
59. Sandoval, M.A.; Fuentes, R.; Nava, J.L.; Rodríguez, I. Fluoride removal from drinking water by electrocoagulation in a continuous filter press reactor coupled to a flocculator and clarifier. *Sep. Purif. Technol.* **2014**, *134*, 163–170. [[CrossRef](#)]
60. Castañeda, L.F.; Coreño, O.; Nava, J.L.; Carreño, G. Removal of fluoride and hydrated silica from underground water by electrocoagulation in a flow channel reactor. *Chemosphere* **2020**, *244*, 125417. [[CrossRef](#)] [[PubMed](#)]
61. Chibania, A.; Barhoumia, A.; Nciba, S.; Bouguerra, W.; Elalouia, E. Fluoride removal from synthetic groundwater by electrocoagulation process: Parametric and energy evaluation. *Desalination Water Treat.* **2019**, *157*, 100–109. [[CrossRef](#)]
62. Ghosh, D.; Medhi, C.; Purkait, M. Techno-economic analysis for the electrocoagulation of fluoride-contaminated drinking water. *Toxicol. Environ. Chem.* **2011**, *93*, 424–437. [[CrossRef](#)]
63. Guzmán, A.; Nava, J.L.; Coreño, O.; Rodríguez, I.; Gutiérrez, S. Arsenic and fluoride removal from groundwater by electrocoagulation using a continuous filter-press reactor. *Chemosphere* **2016**, *144*, 2113–2120. [[CrossRef](#)]
64. Sandoval, M.A.; Fuentes, R.; Thiam, A.; Salazar, R. Arsenic and fluoride removal by electrocoagulation process: A general review. *Sci. Total Environ.* **2020**, 142108. [[CrossRef](#)]
65. Shen, F.; Chen, X.; Gao, P.; Chen, G. Electrochemical removal of fluoride ions from industrial wastewater. *Chem. Eng. Sci.* **2003**, *58*, 987–993. [[CrossRef](#)]
66. Silva, J.F.; Graça, N.S.; Ribeiro, A.M.; Rodrigues, A.E. Electrocoagulation process for the removal of co-existent fluoride, arsenic and iron from contaminated drinking water. *Sep. Purif. Technol.* **2018**, *197*, 237–243. [[CrossRef](#)]
67. Thakur, L.S.; Goyal, H.; Mondal, P. Simultaneous removal of arsenic and fluoride from synthetic solution through continuous electrocoagulation: Operating cost and sludge utilization. *J. Environ. Chem. Eng.* **2019**, *7*, 102829. [[CrossRef](#)]
68. Hu, C.-Y.; Lo, S.-L.; Kuan, W.-H. Simulation the kinetics of fluoride removal by electrocoagulation (EC) process using aluminum electrodes. *J. Hazard. Mater.* **2007**, *145*, 180–185. [[CrossRef](#)] [[PubMed](#)]
69. Mameri, N.; Yeddou, A.; Lounici, H.; Belhocine, D.; Grib, H.; Bariou, B. Defluoridation of septentrional Sahara water of North Africa by electrocoagulation process using bipolar aluminium electrodes. *Water Res.* **1998**, *32*, 1604–1612. [[CrossRef](#)]
70. Emamjomeh, M.M.; Sivakumar, M. An empirical model for defluoridation by batch monopolar electrocoagulation/flotation (ECF) process. *J. Hazard. Mater.* **2006**, *131*, 118–125. [[CrossRef](#)] [[PubMed](#)]
71. Vasudevan, S.; Kannan, B.S.; Lakshmi, J.; Mohanraj, S.; Sozhan, G. Effects of alternating and direct current in electrocoagulation process on the removal of fluoride from water. *J. Chem. Technol. Biotechnol.* **2011**, *86*, 428–436. [[CrossRef](#)]
72. Essadki, A.H.; Gourich, B.; Azzi, M.; Vial, C.; Delmas, H. Kinetic study of defluoridation of drinking water by electrocoagulation/electroflotation in a stirred tank reactor and in an external-loop airlift reactor. *Chem. Eng. J.* **2010**, *164*, 106–114. [[CrossRef](#)]
73. Bennajah, M.; Maalmi, M.; Darmane, Y.; Touhami, M.E. Defluoridation of drinking water by electrocoagulation/electroflotation: Kinetic study. *J. Urban Environ. Eng.* **2010**, *4*, 37–45. [[CrossRef](#)]
74. Betancor-Abreu, A.; Mena, V.; González, S.; Delgado, S.; Souto, R.; Santana, J. Design and optimization of an electrocoagulation reactor for fluoride remediation in underground water sources for human consumption. *J. Water Process Eng.* **2019**, *31*, 100865. [[CrossRef](#)]
75. Hakizimana, J.N.; Gourich, B.; Chafi, M.; Stiriba, Y.; Vial, C.; Drogui, P.; Naja, J. Electrocoagulation process in water treatment: A review of electrocoagulation modeling approaches. *Desalination* **2017**, *404*, 1–21. [[CrossRef](#)]
76. Changmai, M.; Pasawan, M.; Purkait, M. A hybrid method for the removal of fluoride from drinking water: Parametric study and cost estimation. *Sep. Purif. Technol.* **2018**, *206*, 140–148. [[CrossRef](#)]
77. Hashim, K.S.; Shaw, A.; Al Khaddar, R.; Pedrola, M.O.; Phipps, D. Defluoridation of drinking water using a new flow column-electrocoagulation reactor (FCER)-Experimental, statistical, and economic approach. *J. Environ. Manag.* **2017**, *197*, 80–88. [[CrossRef](#)] [[PubMed](#)]
78. Oulebsir, A.; Chaabane, T.; Zaidi, S.; Omine, K.; Alonzo, V.; Darchen, A.; Msagati, T.; Sivasankar, V. Preparation of mesoporous alumina electro-generated by electrocoagulation in NaCl electrolyte and application in fluoride removal with consistent regenerations. *Arab. J. Chem.* **2020**, *13*, 271–289. [[CrossRef](#)]
79. Hu, C.; Lo, S.; Kuan, W. Effects of co-existing anions on fluoride removal in electrocoagulation (EC) process using aluminum electrodes. *Water Res.* **2003**, *37*, 4513–4523. [[CrossRef](#)]
80. Thakur, L.S.; Mondal, P. Techno-economic evaluation of simultaneous arsenic and fluoride removal from synthetic groundwater by electrocoagulation process: Optimization through response surface methodology. *Desalination Water Treat.* **2016**, *57*, 28847–28863. [[CrossRef](#)]
81. Reynolds, T.D.; Richards, P.A.C. *Unit Operations and Processes in Environmental Engineering*; PWS Publishing Company: Boston, MA, USA, 1995.
82. Graça, N.S.; Ribeiro, A.M.; Rodrigues, A.E. Removal of fluoride from water by a continuous electrocoagulation process. *Ind. Eng. Chem. Res.* **2019**, *58*, 5314–5321. [[CrossRef](#)]
83. Ghosh, D.; Medhi, C.; Purkait, M. Treatment of fluoride containing drinking water by electrocoagulation using monopolar and bipolar electrode connections. *Chemosphere* **2008**, *73*, 1393–1400. [[CrossRef](#)]

84. Pulkka, S.; Martikainen, M.; Bhatnagar, A.; Sillanpää, M. Electrochemical methods for the removal of anionic contaminants from water—A review. *Sep. Purif. Technol.* **2014**, *132*, 252–271. [[CrossRef](#)]
85. Ghanizadeh, G.; Shariatineghab, G.; Salem, M.; Khalagi, K. Taguchi experimental design for electrocoagulation process using alternating and direct current on fluoride removal from water. *Desalination Water Treat.* **2016**, *57*, 12675–12683. [[CrossRef](#)]
86. Hu, C.-Y.; Lo, S.-L.; Kuan, W.-H.; Lee, Y.-D. Treatment of high fluoride-content wastewater by continuous electrocoagulation–flotation system with bipolar aluminum electrodes. *Sep. Purif. Technol.* **2008**, *60*, 1–5. [[CrossRef](#)]
87. Rosales, M.; Coreño, O.; Nava, J.L. Removal of hydrated silica, fluoride and arsenic from groundwater by electrocoagulation using a continuous reactor with a twelve-cell stack. *Chemosphere* **2018**, *211*, 149–155. [[CrossRef](#)]
88. WHO. *Aluminium in Drinking-Water: Background Document for Development of WHO Guidelines for Drinking-Water Quality*; World Health Organization: Geneva, Switzerland, 2003; Available online: <https://apps.who.int/iris/handle/10665/75362> (accessed on 15 February 2021).
89. Mouedhen, G.; Feki, M.; Wery, M.D.P.; Ayedi, H.F. Behavior of aluminum electrodes in electrocoagulation process. *J. Hazard. Mater.* **2008**, *150*, 124–135. [[CrossRef](#)]
90. Koparal, A.S.; Ögütveren, Ü.B. Removal of nitrate from water by electroreduction and electrocoagulation. *J. Hazard. Mater.* **2002**, *89*, 83–94. [[CrossRef](#)]
91. Yilmaz, A.E.; Boncukcuoğlu, R.; Kocakerim, M.M. An empirical model for parameters affecting energy consumption in boron removal from boron-containing wastewaters by electrocoagulation. *J. Hazard. Mater.* **2007**, *144*, 101–107. [[CrossRef](#)] [[PubMed](#)]
92. Yilmaz, A.E.; Boncukcuoğlu, R.; Kocakerim, M.M.; Yilmaz, M.T.; Paluluoğlu, C. Boron removal from geothermal waters by electrocoagulation. *J. Hazard. Mater.* **2008**, *153*, 146–151. [[CrossRef](#)] [[PubMed](#)]
93. Takdastan, A.; Emami Tabar, S.; Neisi, A.; Eslami, A. Fluoride removal from drinking water by electrocoagulation using iron and aluminum electrodes. *Jundishapur J. Health Sci.* **2014**, *6*. [[CrossRef](#)]
94. Bhagawan, D.; Saritha, P.; Shankaraiah, G.; Himabindu, V. Fluoride Removal from Groundwater Using Hybrid Cylindrical Electrocoagulation Reactor. *J. Water Chem. Technol.* **2019**, *41*, 164–169. [[CrossRef](#)]
95. Khan, S.U.; Asif, M.; Alam, F.; Khan, N.A.; Farooqi, I.H. Optimizing Fluoride Removal and Energy Consumption in a Batch Reactor Using Electrocoagulation: A Smart Treatment Technology. In *Smart Cities—Opportunities and Challenges*; Springer: Singapore, 2020; pp. 767–778. [[CrossRef](#)]
96. Lacson, C.F.Z.; Lu, M.-C.; Huang, Y.-H. Fluoride containing water: A global perspective and a pursuit to sustainable water defluoridation management—an overview. *J. Clean. Prod.* **2020**, 124236. [[CrossRef](#)]
97. Gürses, A.; Yalçın, M.; Doğar, C. Electrocoagulation of some reactive dyes: A statistical investigation of some electrochemical variables. *Waste Manag.* **2002**, *22*, 491–499. [[CrossRef](#)]
98. Sandoval, M.A.; Fuentes, R.; Nava, J.L.; Coreño, O.; Li, Y.; Hernández, J.H. Simultaneous removal of fluoride and arsenic from groundwater by electrocoagulation using a filter-press flow reactor with a three-cell stack. *Sep. Purif. Technol.* **2019**, *208*, 208–216. [[CrossRef](#)]
99. Gwala, P.; Andey, S.; Mhaisalkar, V.; Labhasetwar, P.; Pimpalkar, S.; Kshirsagar, C. Lab scale study on electrocoagulation defluoridation process optimization along with aluminium leaching in the process and comparison with full scale plant operation. *Water Sci. Technol.* **2011**, *63*, 2788–2795. [[CrossRef](#)]
100. Luna, J.; Martinez, J.; Montero, C.; Muñoz, C.; Ortiz, J.; Gonzalez, G.; Vazquez, V.; Equihua, F. Defluoridation of groundwater in central Mexico by electrocoagulation. *Fluoride* **2018**, *51*, 34–43.
101. Wali, A.; Saidutta, M. Defluoridation of Fresh Water Using the Process of Electrocoagulation Combined with Adsorption. *Int. J. Earth Sci. Eng.* **2013**, *6*, 673–678.
102. Jalil, S.; Amri, N.; Ajien, A.; Ismail, N.; Ballinger, B. A hybrid electrocoagulation-adsorption process for fluoride removal from semiconductor wastewater. *J. Phys. Conf. Ser.* **2019**, 12056. [[CrossRef](#)]
103. Zhao, H.-Z.; Yang, W.; Zhu, J.; Ni, J.-R. Defluoridation of drinking water by combined electrocoagulation: Effects of the molar ratio of alkalinity and fluoride to Al (III). *Chemosphere* **2009**, *74*, 1391–1395. [[CrossRef](#)] [[PubMed](#)]
104. Kashi, G.; Nasehi, N. Fluoride removal from drinking water using the combination of electro and chemical coagulation processes. *J. Health Field* **2017**, *2*. [[CrossRef](#)]
105. Essadki, A.H.; Gourich, B.; Vial, C.; Delmas, H.; Bennajah, M. Defluoridation of drinking water by electrocoagulation/electroflotation in a stirred tank reactor with a comparative performance to an external-loop airlift reactor. *J. Hazard. Mater.* **2009**, *168*, 1325–1333. [[CrossRef](#)] [[PubMed](#)]